https://doi.org/10.15407/ufm.22.03.307

V.A. DEKHTYARENKO*, D.G. SAVVAKIN, V.I. BONDARCHUK, V.M. SHYVANYUK***, T.V. PRYADKO, and O.O. STASIUK**

G.V. Kurdyumov Institute for Metal Physics of the N.A.S. of Ukraine,
36 Academician Vernadsky Blvd., UA-03142 Kyiv, Ukraine

*devova@i.ua, ** savva@imp.kiev.ua, *** shyva@imp.kiev.ua

$TiMn_2$-BASED INTERMETALLIC ALLOYS FOR HYDROGEN ACCUMULATION: PROBLEMS AND PROSPECTS

The main advantages of hydrogen as an energy carrier in comparison with currently used hydrocarbons are determined. By comparing the advantages and disadvantages of available methods of hydrogen storage, it was proved that storage of it in a bound state (hydrides) provides the largest amount of stored hydrogen per unit weight of the container and is the safest method. As shown, the alloys based on AB_2-type intermetallics are the most promising materials for safe storage and transportation of hydrogen in the bound state.

Keywords: hydrogen, hydrides, Laves phase, hydrogenation, dehydrogenation, hydrogen capacity.

1. Introduction

The basis of modern world power production is non-renewable energy sources (oil, gas, and coal) whose reserves are limited, which requires the search for new alternative sources and technologies for energy production. Thanks to scientific and technological progress, humanity has already entered a transition period from energy based on organic natural resources to renewable sources, which are virtually inexhaustible. The main reasons for the importance of the fastest transition to alternative energy sources are environmental, economic, and social factors.

Alternative energy sources are based on the use of natural resources, such as solar energy, wind and sea waves; hydrogen energy also

Citation: V.A. Dekhtyarenko, D.G. Savvakin, V.I. Bondarchuk, V.M. Shyvanyuk, T.V. Pryadko, and O.O. Stasiuk, $TiMn_2$-Based Intermetallic Alloys for Hydrogen Accumulation: Problems and Prospects, *Progress in Physics of Metals*, **22**, No. 3: 307–351 (2021)

takes an important place in this list. Hydrogen economy favourably differs from other alternative methods, since today only it can be most effectively used 'on board' in vehicles. The choice of hydrogen [1, 2] as an energy source is due to a number of significant advantages over hydrocarbons (see Table 1). According to Ref. [2], in addition to the benefits listed in Table 1, one should also take into account virtually unlimited stocks of raw materials if hydrogen production from water is considered (the hydrosphere contains $1.39 \cdot 10^{18}$ tons of water). Environmental safety of hydrogen (the product of its combustion is water) and its low viscosity are also very important at transportation through pipelines [2].

However, today, there are a number of problems in the hydrogen economy, that constrain its practical implementation, and their solution has significant economic and environmental importance. One of the main tasks is to find scientific and technological solutions for convenient storage and transportation of hydrogen. Solution of this problem will give impetus to the further development of the use of hydrogen energy sources [3, 4]. Conventional storage methods developed for liquid and gaseous hydrogen are unacceptable in a wide range of cases for a number of reasons: high pressure, significant mass and volume of containers per unit mass of hydrogen stored, high energy consumption for liquefaction [5–7].

According to the literature [2, 4, 8–15], it is now proven that it is more profitable and safer to store hydrogen in the bound state than in the liquid or gaseous state (Table 2). There are two main types of hydrogen storage in the bound state: (i) adsorption methods, and (ii) storage in the form of metal hydrides.

In adsorption methods, the accumulation of hydrogen occurs in zeolites and carbon materials of different morphology (activated carbon, nanotubes, nanofibres and polymers), as well as in highly porous metal–organic frameworks [2]. However, the main disadvantage of these materials as hydrogen sorbents is that they can only work at low temperatures $\approx$70 K. Besides, their hydrogen absorption properties largely depend on the surface roughness, so the amount of absorbed hydrogen does not exceed 2.0 wt.%.

Despite the fact that all the proposed methods of hydrogen storage have already found their application in production, the majority of researchers [16–18] came to the conclusion that the most promising solution is still the use of solid compounds (metal hydrides) as convenient materials for the accumulation, release, storage and transportation of hydrogen [19–23]. For this class of metallic materials, the volume of hydrogen absorbed is several orders of magnitude higher than the volume of the original alloy; however, they should meet a number of requirements. Metallic materials used as hydrogen accumulators should

provide the inversion of hydrogen absorption and desorption and an easy control of these processes by changing thermal or pressure conditions, have high hydrogen capacity and rate of reaction with hydrogen. In addition, an important characteristic of these materials, especially for the use as mobile energy sources, is their low specific weight.

According to the literature [8, 24], the process of interaction of metallic materials with hydrogen (Fig. 1) is quite complex and can be divided into the following main stages:

• contact of molecular hydrogen with metal surface;

• accumulation of hydrogen molecules on the surface and their dissociation (physical adsorption, dissociation and chemical adsorption (chemisorption) of hydrogen molecules);

• redistribution of H atoms in the volume of metal (diffusion);

• ordered arrangement of hydrogen atoms in the interstices of the metal matrix with progressive formation of hydride.

The absorption (dissolution, absorption) of hydrogen by metal usually means the transition of hydrogen from the gaseous state into the metal. The term 'absorbed hydrogen' means all the absorbed hydrogen

Table 1. **Characteristics of different types of fuel [2]**

Parameter	Hydrogen	Methane	Petrol
Lower heating value, kW·h/kg	33.33	13.9	12.4
Autoignition temperature, °C	585	540	228–501
Flame temperature, °C	2045	1875	2200
Flammability limits in air, vol.%	4–75	5.3–15	1.0–7.69
Lower flammability energy, mV/s	0.02	0.29	0.24
Flame propagation velocity in air, m/s	2.65	0.4	0.4
Coefficient of diffusion in air, cm^2/s	0.61	0.16	0.05
Toxicity	—	—	high

Table 2. **Comparison of different ways of hydrogen storage [2]**

Hydrogen state	Specific capacity			Operating temperature, K	Pressure, MPa
	kg H_2/dm^3	kW·h/kg	kW·h/dm^3		
Liquid	71	33.3	2.36	20.4	0.1–0.4
Gaseous in cylinders:					
steel	9–18	33.3	0.15–0.3	210–330	10–20
reinforced aluminium	9–18	33.3	0.15–0.3	210–330	10–20
composite materials	30	33.3	0.3	210–330	70
Hydrides:					
low-temperature	96	0.58	3.2	260–370	0.1–3
high-temperature	81–101	1.05–2.3	2.7–3.4	>500–600	0.1–3

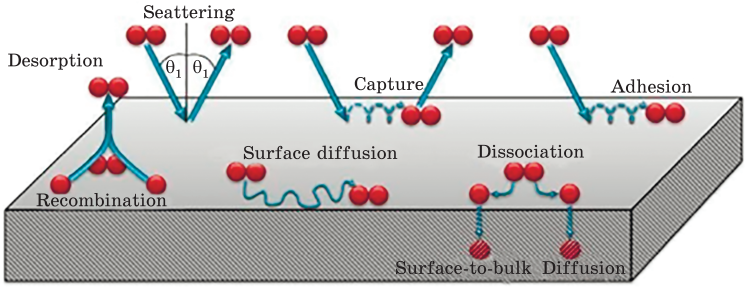

Fig. 1. Scheme of reactions on the hydrogen/metal interface [24]

in both solid solution and in the form of a chemical compound (hydride). The hydrogen capacity is the maximum amount of hydrogen that a certain metallic material is able to absorb.

As noted in work [24] based on the data of Ref. [25], there are no specific forces that cause hydrogen adsorption. Nevertheless, it was explained that the adsorption of hydrogen molecules by the metal surface occurs due to attractive forces between molecular hydrogen and the surface atoms of the adsorbent. Hydrogen molecules can be adsorbed on the metal surface due to physical or chemical adsorption. The authors of [24] claim that physical adsorption is caused by the Van der Waals interaction between molecular hydrogen and adsorbent atoms, and a hydrogen molecule simultaneously interacts with several atoms of the adsorbent (Fig. 1). The potential energy of a hydrogen molecule has a minimum at a distance of approximately one radius of the adsorbent molecule (0.2 nm) [26, 27]. The energy of physical adsorption is usually negative, and its modulus does not exceed 20 kJ/mol H (−0.2 eV). For many metals, the energy of physical adsorption is close to −5 kJ/mol H (−0.05 eV) [26], so significant physical adsorption occurs only at low temperatures (<273 K) [27, 28].

The next stage in the metal–hydrogen interaction (*Me*–H) is the dissociation of a hydrogen molecule into atoms, since only atomic hydrogen is able to overcome the energy barrier and get into the volume of the metal from its surface. This process is called chemisorption; its energy is usually negative in the range from −20 to −400 kJ/mol H, and for many metals, it equals −50 kJ/mol H [26]. According to the authors of [24], at the last stage, an ordered arrangement of hydrogen atoms in the interstices of the metal matrix with the formation of a hydride of a certain stoichiometry occurs. In Ref. [29], it was clarified that this is possible only in cases when the interstice radius is greater than 0.4 Å (which is related to the size of a hydrogen atom that should fit there), and the distance between hydrogen atoms located in adjacent interstices is more than 1.8 Å.

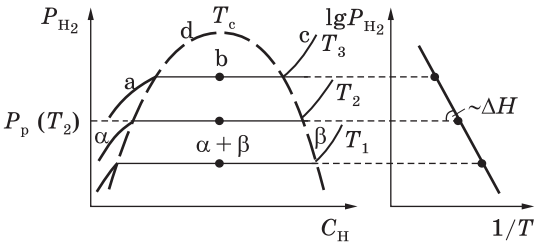

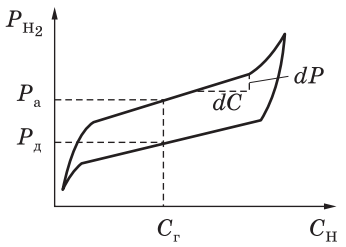

Fig. 2. Pressure–temperature phase diagram of a metal–hydrogen system [2]

Fig. 3. Hysteresis and slope of the pressure plateau on the (pressure–concentration) *p*–*C* isotherms [2]

However, the process of hydride formation is rather complex. According to the data presented in [2, 30], the process of hydride phase formation can be explained based on experimental pressure-composition isotherms (Fig. 2).

As shown in Fig. 2, at the initial stage 'a', the pressure as a function of the hydrogen content in the metal increases quite rapidly, which corresponds to the formation of α-solid solution of hydrogen in the metal. Upon further interaction with hydrogen, α-solid solution becomes saturated at certain pressure and concentration, and subsequent dissolution of hydrogen leads to the formation of β-hydride phase. In this diagram (Fig. 2), the stage of hydride formation corresponds to the horizontal section 'b', which corresponds to the α↔β-transformation plateau. This is because, according to the Gibbs phase rule, the formation of β-hydride is an invariant equilibrium and should ideally occur at constant pressure [2]. The end of the horizontal section corresponds to the completion of the hydride formation process. Further increase in pressure with hydrogen concentration corresponds to the dissolution of hydrogen in the hydride phase (section 'c'). That is why, in real systems, an increase of the pressure on the plateau leads to longer times needed for the formation of supersaturated α-solid solution, reducing the overall rate of interaction with hydrogen, and requires higher reaction pressures.

Many authors [8–15] note that the process of hydride formation described above is rather speculative, while in real systems a pressure hysteresis is always observed (see Fig. 3).

Hydrogen absorption always occurs at a higher pressure than its desorption that is explained by residual plastic deformation caused by rapid changes in the crystal lattice volume during the reverse transition from saturated α-solid solution to β-hydride [2]. In real systems, the horizontal plateau corresponding to the α↔β-transformation is often absent (Fig. 3), and the degree of deviation from the horizontal can be significant, depending on the material. The increase in hysteresis leads

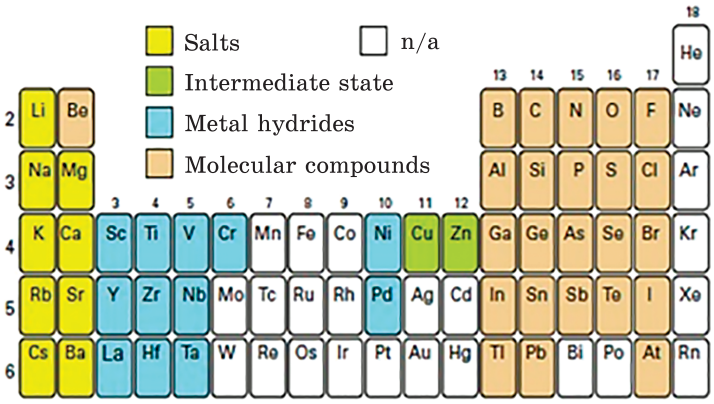

Fig. 4. Classification of hydrogen–material compounds in the periodic table [24]

to a deterioration of the process of hydrogen desorption, which is an important issue in the practical use of hydrides as hydrogen sorbents.

In Ref. [29], the metals capable of forming metal hydrides were considered (Fig. 4), and the changes in their structure upon the interaction with hydrogen were investigated. As found, the dissolution of hydrogen in the metal lattice can lead to the following:

• fundamental restructuring of the metal lattice, for example, the transition from body-centred cubic (b.c.c.) to face-centred cubic (f.c.c.) structure in the hydride sublattice;

• no significant changes in the structure can occur; in this case, the type of metallic lattice in the hydride zones does not differ from that of the initial metal (except the deformation of the unit cell).

However, the important question was whether all metallic materials are equally capable of interacting with hydrogen and forming chemical compounds with it (hydrides). In Refs. [24, 31], all *Me*–H (hydrogen–material) compounds were divided into three main classes, based on the nature of the formed chemical bonds according to the common classification (Fig. 4): (i) ionic (saline) hydrides, (ii) metal hydrides, and (iii) covalent hydrides (molecular compounds).

As clearly seen in Fig. 4, only part of the metals in the periodic table of the elements is able to interact with hydrogen and form metal hydrides (marked in blue). According to Ref. [2], elements such as manganese, iron and cobalt do not interact with hydrogen, whereas, as noted [24, 31], the possibility of interaction with hydrogen is currently unknown for a large group of metals (white). According to the literature [2, 4], it is proved that by the combination in certain crystal-chemical compounds (*e.g.*, intermetallics) of two (or even more) metals which have significantly different activity with respect to hydrogen (Fig. 4) (*e.g.*,

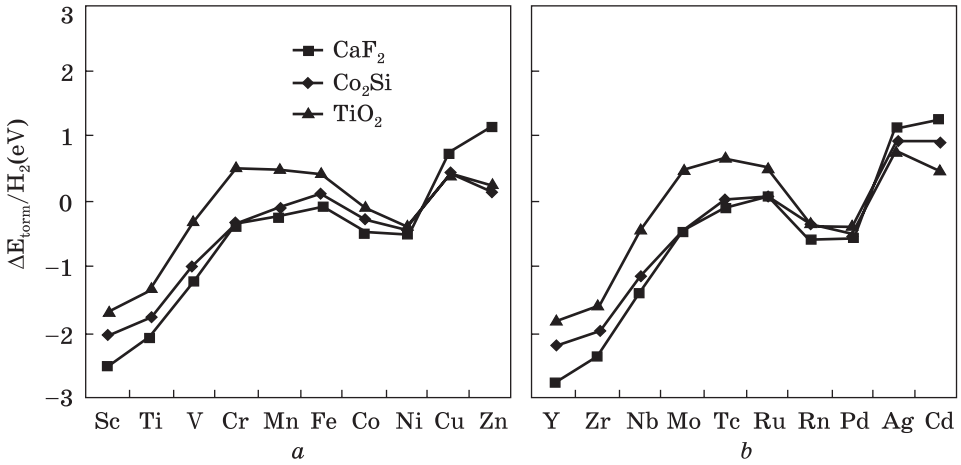

Fig. 5. Change of dihydride formation energy for 3*d*- and 4*d*-metals [36]

titanium and manganese) it is possible to create compositions that significantly outperform the source metals in hydrogen absorption properties.

Based on the data presented of [32–35] and the calculations of the electronic structure of hydrides (monohydrides), the changes in the free energy of dihydride formation for 3*d*- and 4*d*-metals was determined in Ref. [36] using calculations from the first principles (Fig. 5). The authors claim that this reaction is thermodynamically beneficial for the system only in the cases when the interaction of 3*d*- or 4*d*-metals with hydrogen is accompanied by negative changes in the free energy (Fig. 5). Accordingly, the elements with a negative change in energy are able to form a stable chemical compound with hydrogen (hydride) (Figs. 4 and 5). The results obtained in [36] coincide with the data of [24] in that the ability of 3*d*- and 4*d*-metals to form stable chemical compounds with hydrogen sharply decreases when we shift in the table of elements from left to right.

2. The Main Types of Materials for Storing Hydrogen in Bound State and Prospects for Their Application

The current level of development of hydrogen materials allows selecting appropriate materials with properties needed for concrete technical problems: temperature and pressure of synthesis and decomposition of hydrides, thermodynamic and kinetic characteristics of hydride formation processes [37–39]. Table 3 classifies the known hydrogen absorbing metallic materials, basing on their structure, the amount of absorbed hydrogen, and the characteristics of the hydrogenation and dehydrogenation processes [2, 4].

Such materials primarily include magnesium and magnesium-based alloys, titanium and titanium-based b.c.c. solid solutions, as well as intermetallic compounds. Each type of currently existing hydrogen accumulating materials has both some advantages and disadvantages, which are described below.

The main advantages of magnesium as a hydrogen-accumulating material include the possibility of obtaining a hydride by hydrogenating this metal in a hydrogen gas environment, as well as the highest amount of sorbed hydrogen (7.67 wt.%) among the known materials [40]. However, the process of obtaining magnesium hydride is difficult and requires the use of stringent thermobaric conditions for its implementation, and complex activation treatment. In addition, the stability of magnesium hydride is insufficient upon multiple cycles of sorption–desorption, which leads to gradual loss of the required characteristics.

As a material for storing hydrogen, magnesium has a very low rate of interaction with hydrogen, especially upon the first hydrogenation, which is the most problematic moment. This is due to the formation of a thin layer of magnesium hydride on the surface of the particles, which inhibits the diffusion of hydrogen atoms into the metal volume. According to [41], the first hydrogenation of magnesium at a temperature of 340–350 °C and hydrogen pressure up to 3 MPa can be completed within 6–336 hours. These large differences in the time of interaction with hydrogen are explained by the high sensitivity of the reaction rate, varying particle size, surface conditions of the initial metal, activation conditions, and purity of hydrogen gas. The reaction can be accelerated by increasing the hydrogenation temperature up to 400–450 °C and hydrogen pressure up to 10–20 MPa, in combination with some catalysts. However, instead of the effect of pressure and temperature on the kinetics of the sorption process, mechanical activation treatment (*e.g.*,

Table 3. **Characteristics of different types of hydrogen absorbing alloys [2, 4]**

Type	Alloy	Capacity		Operating temperature range, °C	Dissociation pressure, atm	Hydrogenation rate	Activation conditions
		H/*Me*	wt.%				
AB_5	$LaNi_5$ $MnNi_5$	1.4	0.8–1.2	Ambient	0.5–15	high	mild
AB_2 (Laves phases)	$ZrMn_2$ $TiMn_2$ ZrV_2	1.3	1.5–2.0	Ambient	0.5–20	"	"
AB	TiFe	1.2	1.4–1.81	Ambient	0.5–15	low	severe
(b.c.c.)	Ti–V	2.0	3.9–4.0	400–600	1–15	"	"
(Mg)	Mg–Ni	2.0	6.5–7.67	350–450	1–10	"	"

grinding of magnesium in a ball mill) under hydrogen pressure is widely used that is also an effective method for enhancing the absorption kinetics of hydrogen [42].

As found [40], some other methods of plastic deformation of magnesium and magnesium-based alloys allow to enhance significantly the kinetics of the first hydrogenation. Particularly, equal-channel angular pressing of large ingots of magnesium alloys with their subsequent dispersion into powder was as effective as prolong grinding in a ball mill for accelerating the kinetics of hydrogenation [43, 44]. The positive effect of torsion under high pressure on the kinetics of the hydrogenation process and on the decrease in the temperature of the beginning of active absorption was also demonstrated [45]. The main problem of the proposed methods of enhancing the kinetics of hydrogenation of magnesium is their technological complexity, high cost and, especially, difficulties in producing large amounts of material with the necessary properties in moving from laboratory scale to production [40]. According to the literature [46], magnesium-based hydride has a high thermal stability, which is a negative feature for practical use. For example, it is necessary to heat magnesium hydride to rather high temperature of ≈300 °C to provide a hydrogen pressure of 0.1 MPa.

Beside the above-mentioned shortcomings associated with the kinetics of sorption–desorption processes, magnesium and magnesium-based alloys have poor cyclic stability, which results in the degradation of hydrogen absorption properties with hydrogenation-dehydrogenation cycles. Although the literature data on the cyclic stability are quite contradictory (most likely due to different experimental conditions), the effects of degradation during cycling have been recorded, which were associated with partial irreversible loss of absorbed hydrogen [47] and the deterioration of the kinetics of hydrogen sorption–desorption, especially at lower temperatures [48]. Given all these advantages and disadvantages, magnesium and magnesium-based alloys are currently very strictly used as sorbent materials in autonomous or stationary hydrogen storage systems.

The main advantages of titanium or b.c.c. titanium-based solid solutions as hydrogen-accumulating materials are the possibility of forming a hydride by a direct hydrogenation reaction in a hydrogen gas environment and a fairly high amount of absorbed hydrogen (up to 4 wt.%) [49, 50], but the process of obtaining titanium hydride and its decomposition, as for magnesium, has a number of shortcomings.

According to the literature [49–51], titanium hydride can be obtained by heating the metal in pre-evacuated furnaces under hydrogen pressure, followed by exposure at temperatures of 400–600 °C in a gas atmosphere. However, as the authors note, this process of titanium hydrogenation takes several hours, which is associated with the gradual

diffusive saturation of the crystal lattice by hydrogen, and therefore requires significant energy costs. Besides, the significant duration of the process noticeably increases the risk of contamination of the hydrides with impurities (oxygen, nitrogen) from the residual atmosphere in the vacuum furnace, which negatively affects both the amount of hydrogen absorbed and the sorption–desorption kinetics.

As shown in works [52, 53], the process of decomposition of titanium hydride, as well as the process of its production, require significant energy costs. The authors claim that at a relatively slow (7 °C/min) heating at the initial pressure of 10^{-4} Pa in the chamber titanium hydride starts to desorb hydrogen above 300 °C, and this process completes at 600 °C. In addition, they also noted that the completion temperature of the process of hydrogen desorption from titanium hydride was significantly affected by the heating rate. It was shown that at high heating rates (20 °C/min and more) the completion temperature of the hydrogen desorption process shifted towards higher values, and the process ended at hydrogen content of 0.01 wt.% at the temperatures of 1250–1350 °C. The processes of forming titanium hydride and its decomposition require heating to high temperatures and long-term exposure; therefore, titanium or titanium-based b.c.c. solid solutions are practically not used as sorbent materials for hydrogen accumulation in autonomous and mobile hydrogen storage systems.

In contrast to titanium and magnesium, intermetallics are characterized by a relatively low amount of absorbed hydrogen—up to 2.0 wt.% [54, 55]; nevertheless, they are able to interact at high rates with hydrogen at room temperature without the use of pre-activation thermal vacuum or mechanical treatment. The process of decomposition of the formed hydrides does not require large energy costs (in intermetallics, it is possible to desorb all absorbed hydrogen at a temperature of 350 °C [56]). However, the main disadvantage of intermetallics, which limited their practical use in vehicles for a long time, was their low hydrogen capacity compared to magnesium and titanium-based b.c.c. solid solutions [57, 58]. At present, this disadvantage has been used as an advantage in practical use in freight transport (replacement of the standard counterweight with a hydrogen battery) [59, 60].

The importance of the rate of interaction of the material with hydrogen and the temperatures of hydrogen sorption–desorption in comparison with the hydrogen capacity is explained by the fact that, in practical use in transport, it is very important to minimize time and energy to recharge a hydrogen battery.

According to the data listed in Table 3, intermetallics used in mobile or stationary hydrogen storage systems are divided into three main types AB_5, AB, and AB_2, where the main representative compounds are as follow: $LaNi_5$ [61, 62], TiFe [63, 64], and $TiMn_2$ [65, 66], respec-

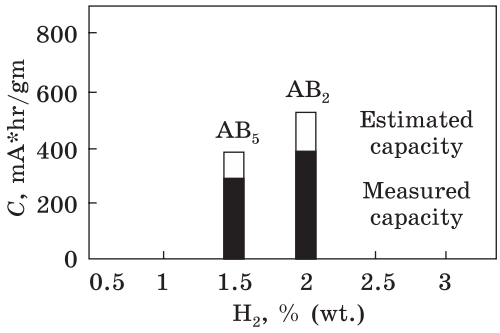

Fig. 6. Comparison of discharge and hydrogen capacities of AB_5- and AB_2-type intermetallides [2]

tively. Each of these intermetallic compounds has significantly different hydrogen sorption properties, which determines the conditions and limits of their practical application.

It was shown in Ref. [67] that the practical application of *AB*-type intermetallics (TiFe), in comparison with the intermetallics of types AB_5 and AB_2, is limited due to the complex activation process of the first hydrogenation. The authors claim that although the process of interaction with hydrogen can occur at room temperature and a pressure of 5 MPa, the rate of absorption reaction is very low. To activate the process of hydrogen absorption during the first hydrogenation in TiFe intermetallic compound, the alloying was proposed in [68, 69] that can significantly affect the rate of interaction with hydrogen. In the study of alloys based on intermetallic compounds TiFe ($TiFeZr_{0.05}$, $Ti_{0.95}FeZr_{0.05}$, and $TiFe_{0.95}Zr_{0.05}$), the authors of Ref. [68] showed that the addition of zirconium can affect the rate of hydrogen absorption during the first hydrogenation. They also claimed that the alloy $TiFe_{0.95}Zr_{0.05}$ (as compared to the intermetallic TiFe and other investigated alloys of this series) had a significantly higher hydrogen capacity. Despite some enhancement in hydrogen absorption characteristics due to alloying, *AB*-type intermetallics are still not used as sorbents in the hydrogen batteries.

An analysis of the literature [70–73] showed that recently for the practical application of hydrogen batteries, especially in transport, the alloys based on the intermetallics of AB_5 or AB_2 type are more promising as hydrogen sorbents.

The authors of Ref. [71] used as a hydrogen sorbent alloy in a metal hydride battery for a forklift an AB_2-type intermetallic compound, and proved that it has significant advantages over the first created for this purpose battery based on an AB_5-type alloy in Ref. [61]. The main advantages of AB_2-based intermetallics are the compactness of the battery and increased operating time without recharging, due to significantly different specific weights of AB_5 and AB_2-type intermetallics and the amount of hydrogen absorbed per unit mass of sorbent material (Fig. 6). In addition, based on previous studies [74], in Ref. [75], the authors showed that in the AB_2-type alloys the rate of interaction with hydrogen is 20–50% higher as compared to the AB_5-type alloys ($LaNi_5$),

which reduces the time required to recharge a hydrogen battery, that is especially important in practical use.

Due to the advantages of materials for hydrogen batteries based on AB_2-type intermetallics, the development and production of new metal compositions based on this type of compounds is especially important.

3. Hydrogen Absorption Properties of AB_2-Type Intermetallics

Among many intermetallics of AB_2-type (Laves phase), the $TiMn_2$ is currently the most widely used in reversible hydrogen storage systems. This is explained by the fact that the $TiMn_2$ intermetallic occupies a special place among the analogues in its class ($ZrMn_2$ and ZrV_2) [2, 4, 30] due to the rapid and simple activation, acceptable kinetic parameters of hydrogen sorption–desorption, a significant amount of absorbed hydrogen ≈1.0 H/*Me* [76, 77] (it was shown in [78] that the unit cell of Laves phase can contain 6 H atoms), high hydrogenation rate [79, 80], a homogeneity region of 11 at.%, and relatively low cost. Another very important advantage, especially when used in transport: in comparison with analogues, $TiMn_2$ has lower specific weight. According to the literature [81–83], $TiMn_2$ (Fig. 7) (Laves phase of *C*14 type) has a hexagonal crystal lattice with the structural type $MgZn_2$ of the spatial group $P6_3/mmc$ (*hP*12 in Pearson symbols). According to [84–86], the lattice parameters in the $TiMn_2$ intermetallic compound linearly change: for *a*, from 0.4812 to 0.4880 nm, and for *c*, from 0.7892 to 0.7992 nm with increasing titanium content from 30 to 41 at.%, respectively.

In Ref. [87], the authors investigated the interaction with hydrogen for binary Ti–Mn system alloys in a region of compositions (59–70 at.% Mn), which correspond to the region of homogeneity of the $TiMn_2$ compound (Fig. 7) [83]. The authors found out that in this region the amount of absorbed hydrogen increased significantly with titanium content. The best kinetic properties of sorption–desorption processes, as well as the maximum possible amount of absorbed hydrogen, were achieved [83] for the alloy Ti–59 at.% Mn, whose composition corresponded to the lower margin of the region of existence of this intermetallic (Fig. 7).

In the work [83], the hydrogen adsorption properties of annealed alloys of the Ti–Mn binary system at 56.4–66.8 at.% Mn were studied, and the results of Ref. [87] were proved: the ability to interact with hydrogen, as well as the amount of absorbed hydrogen in $TiMn_2$-based alloys, strongly depend on their chemical composition. The investigations of the microstructure and phase composition of annealed alloys in this region showed that all the studied alloys were multiphase, and their structure comprised both the intermetallic compounds $TiMn_2$ and TiMn. The presence of the TiMn in the annealed alloys was explained in [83] by the partial decomposition of the $TiMn_2$ intermetallic compound upon

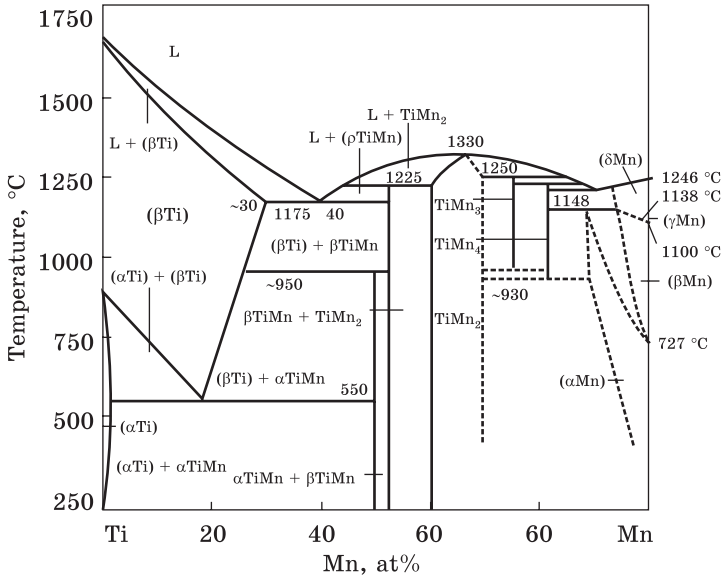

Fig. 7. Phase diagram of Ti–Mn system according to Ref. [83]

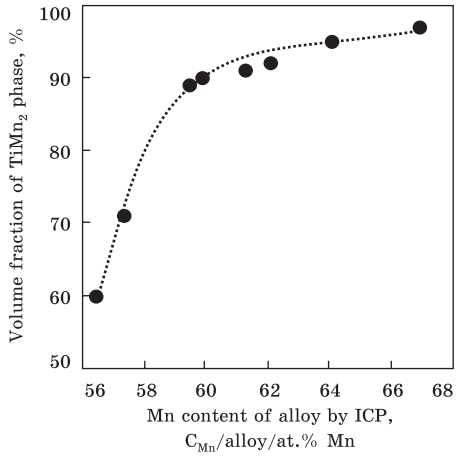

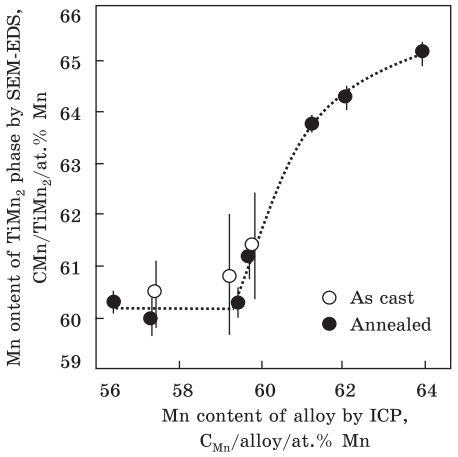

Fig. 8. Dependence of $TiMn_2$ volume fraction on Mn content by inductively coupled plasma (ICP) method [83]

Fig. 9. Dependence of Mn concentration in $TiMn_2$ phase on its content in the as-cast (○) and annealed (●) alloy [83], where SEM–EDS is energy dispersive x-ray spectroscopy in scanning electron microscope (SEM)

heat treatment. Besides, as noted, the volume fraction of the $TiMn_2$ compound for the studied compositions increased with manganese content (Fig. 8). For example, for the Ti–56.4 at.% Mn alloy, the $TiMn_2$ volume fraction was 60%, while, in the Ti–66.8 at.% Mn alloy, it increased up to 97%.

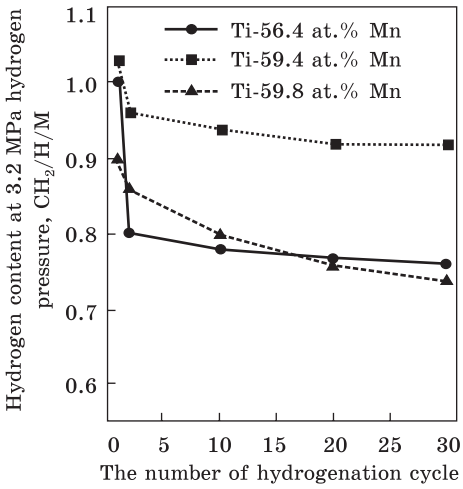

Fig. 10. Dependence of hydrogen concentration on the number of hydrogenation cycles [83]

It was also found out that in the range from 56.4 to 59.4 at.% Mn, the manganese content in the $TiMn_2$ phase was almost constant (60 at.%), whereas, in the alloys Ti–59.4 at.% Mn to Ti–66.8 at.% Mn, the manganese concentration increased from 60 to 66 at.%, respectively (Fig. 9). Although the authors did not mention the reasons for the increase in $TiMn_2$ volume fraction, it can be attributed to the increase of manganese content in this phase, which retards its decomposition upon the thermal treatment.

Hydrogen absorption properties of alloys in the composition range of 56.4–66.8 at.% Mn were investigated at a hydrogen pressure of 3.2 MPa and room temperature. It was shown in Ref. [83] that, at these hydrogenation parameters, the alloys with manganese content from 56.4 to 59.8 at.% absorbed hydrogen at a high rate during the first hydrogenation, whereas the alloys Ti–62.0, Ti–64.0, and Ti–66.8 at.% Mn did not interact with hydrogen at all. Besides, the amount of hydrogen absorbed also differed significantly. For example, in the alloys Ti–56.4 and Ti–59.4 at.% Mn, the amount of absorbed hydrogen increased from $H/Me \approx 0.8$ to 1.0, respectively, while, when the manganese content increased to 61.2 at.% H/Me, there was a sharp decrease to $H/Me \approx 0.2$. These data correlate well with the results of [88]. This difference in the absorption kinetics and the amount of absorbed hydrogen was attributed by the authors to the increase in the amount of manganese in the Laves phase from 60 to 66 at.% in the alloys range from Ti–59.4 to Ti–66.8 at.% Mn. Thus, the authors noted that to achieve in the $TiMn_2$-based alloys both high rate of interaction with hydrogen and hydrogen capacity, these alloys should contain the maximum possible volume fraction of this phase, and, most importantly, the minimum possible manganese content in this phase.

The authors of Ref. [83] also compared the amount of hydrogen absorbed after the first and the second cycle of sorption–desorption process and found that the difference in hydrogen capacity may appear already upon the second hydrogenation. However, they noted that the difference in the amount of hydrogen absorbed during the first and the second cycle decreased with manganese content in the alloy. For exam-

ple, in the Ti–56.4 at.% Mn alloy, the difference in H/*Me* was 0.2, whereas, in the alloys with 59.4–62.0 at.% Mn, it was already absent (Fig. 10). This confirms the authors' conclusion that the amount of hydrogen absorbed during the second hydrogenation cycle increases at higher volume fraction of $TiMn_2$ intermetallic phase and at lower manganese content in the alloy.

In Ref. [88], Ti–60 at.% Mn alloy was studied in a cast state, and the reduction of the amount of absorbed hydrogen with increasing number of sorption–desorption cycles, which was found out in Ref. [83], was investigated in more detail. The experiments were performed by comparing the amount of hydrogen absorbed after the first hydrogenation and after 30 sorption–desorption cycles. The authors noted that, in as-cast state, the alloy consisted mainly of intermetallic $TiMn_2$ phase and of a small amount of intermetallic TiMn phase, which coincides with the data of Ref. [83]. The hydrogenation was performed at a pressure of 3.2 MPa and room temperature, while desorption of hydrogen was investigated by reducing the hydrogen pressure from 3.2 to 0.01 MPa. The authors showed that the amount of absorbed hydrogen abruptly decreased with the number of sorption–desorption cycles (Fig. 10). The authors attributed this to several factors: lattice expansion and its inhomogeneous deformation; Ti-based δ-hydride present in the alloy after hydrogenation. According to [88], complete hydrogen desorption can be achieved only by heating up to 400 °C and 1 h exposure at this temperature.

The appearance δ-hydride (it starts to decompose with hydrogen desorption above 300 °C [52, 53]) leads to higher amount of hydrogen which is not released upon the decomposition of hydride based on $TiMn_2$ intermetallic phase, and thereby residual hydrogen accumulates in the material with each subsequent cycle of sorption-desorption. This leads to decreasing the amount of absorbed and desorbed hydrogen with each subsequent cycle.

Summarizing all the above, we conclude that the main disadvantages of the alloys based on intermetallic $TiMn_2$ compound in binary system Ti–Mn are the high equilibrium pressure plateau, and the hysteresis effect (*i.e.*, the difference between the pressures of hydrogen sorption and desorption) [76].

As shown above, all attempts to improve the sorption–desorption kinetics, as well as to significantly increase the amount of absorbed H in the $TiMn_2$-based intermetallic compounds (the maximum amount of absorbed hydrogen was 1.8 wt.% H/*Me* ≈ 1.0), *via* increasing the number of sorption–desorption cycles, changes in the initial state (as-cast or annealed), or variations in the titanium/manganese ratio (the whole region of $TiMn_2$ on the Ti–Mn binary diagram was investigated [83]) did not lead to a significant improvement in the hydrogen absorption pa-

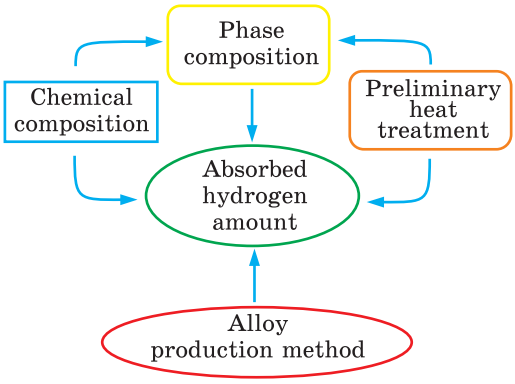

Fig. 11. Scheme demonstrating factors affecting the hydrogen absorption properties of alloys based on $TiMn_2$ intermetallic phase [92]

rameters. According to theoretical calculations [2], hydrogen capacity of AB_2-type intermetallic compounds is 3.9 wt.%, that indicates a significant potential to increase experimentally achieved values of hydrogen capacity in the alloys of this class, and requires further search for ways to enhance hydrogen capacity.

Basing on the data of [2, 76, 83, 88], most researchers concluded that the enhancement of sorption–desorption kinetics and significant increase in the amount of absorbed hydrogen (closer to the theoretical value 3.9 wt.%) will be possible in the $TiMn_2$-based alloys only by additional alloying of this phase [2, 89–91].

Therefore, at present, ternary or even more complex alloying systems on the base of AB_2-type intermetallic compounds are used as hydrogen sorbent materials for transport batteries. In Ref. [2], it was noted that a potential way to increase the hydrogen capacity consists in adding into the material one or even several alloying elements, and at the same time preserving the AB_2-type intermetallic lattice. Potentially, this will allow changing the hydrogen absorption properties of the material in a wide range. This idea determines the importance of the search for chemical elements that can positively affect the kinetics of hydrogen sorption-desorption processes in Ti–Mn alloys with intermetallic AB_2-type lattice, as well as the amount of hydrogen absorbed, and reduce degradation of the properties during sorption-desorption cycling. In Ref. [92], other methods of affecting the amount of hydrogen absorbed were identified in addition to alloying, which are schematically shown in Fig. 11. All these factors are considered separately to determine the most effective of them.

4. Effect of Alloying on Hydrogen Absorption Properties of $TiMn_2$-Based Alloys

In Refs. [93–96], the authors proposed to substitute partially titanium for zirconium (as the component *A*) in the $TiMn_2$ intermetallic phase. They noted that the choice of zirconium as an alloying component is explained by the following factors. First, zirconium has a slightly higher affinity for hydrogen than titanium, so the presence of zirconium in

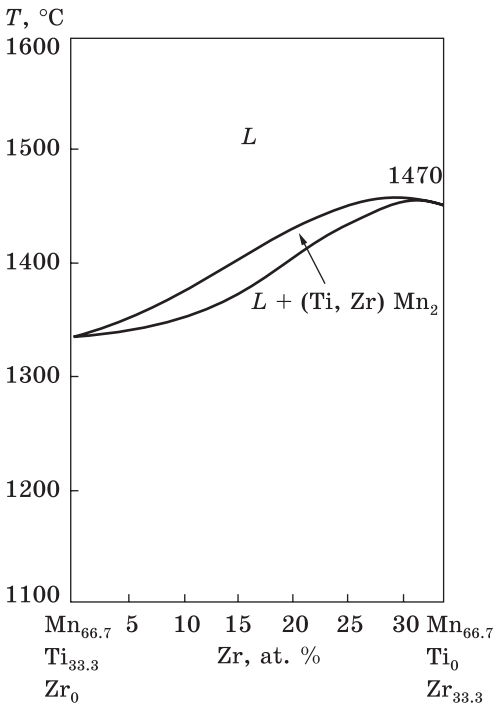

Fig. 12. Quasi-binary section $Zr_{33.3}Mn_{66.7}$–$Ti_{33.3}Mn_{66.7}$ [98]

the alloy can intensify hydrogen absorption. Second, zirconium has a larger atomic radius (0.160 nm) compared to titanium (0.147 nm), and due to this, the partial replacement of titanium atoms in the intermetallic phase $TiMn_2$ by zirconium atoms should increase the parameters of the crystal lattice, and thus, increase the radius of the tetrahedron interstices [92], where dissolved hydrogen atoms are located, that should also lead to higher hydrogen capacity. Third, according to the literature [97, 98], there is a continuous series of solid solutions between the isostructural compounds $TiMn_2$ and $ZrMn_2$ (Fig. 12), *i.e.*, the introduction of zirconium into the $TiMn_2$ intermetallic compound should not cause the formation of new phases; therefore, the three-component material Ti–Zr–Mn will retain the desired type of lattice in a certain concentration range.

The kinetics of sorption–desorption processes were investigated, and the amount of hydrogen absorbed by $Ti_{1-x}Zr_xMn_2$ alloys (x = 0.4; 0.6; 0.8) with AB_2 intermetallic structure at a pressure of 7 MPa and room temperature were determined in Ref. [99]. The amount of absorbed hydrogen H/Me gradually increased from 0.9 to 1.2 with zirconium content in the whole range. Besides, the amount of absorbed hydrogen decreased, and the hydrogenation products became pyrophoric due to powdering after six sorption–desorption cycles. The decrease in the amount of hydrogen absorbed was most likely due to the formation of titanium-based δ-hydride after hydrogenation, as shown in [83]. The process of hydrogen desorption was investigated at room temperature by reducing the hydrogen pressure from 7 MPa to 0.01 MPa; it was found that only a certain chemical composition allowed to obtain a sufficiently high amount of desorbed hydrogen.

The results obtained in [99] on the kinetics of sorption–desorption processes and the amount of absorbed hydrogen (at the H/*Me* level of 0.9–1.2) in $Ti_{1-x}Zr_xMn_2$ ($0 \le x \le 1$) alloys coincided with those presented in [77] for the same hydrogenation parameters, hydrogen pressure of

7 MPa and room temperature. However, the authors noted that significant changes in hydrogenation parameters led to higher hydrogen absorption. As shown, reducing the hydrogen pressure from 7 MPa to 4 MPa and reducing the hydrogenation temperature from 293 K to 80 K in with $0 \le x \le 0.6$ allow to increase the amount of absorbed hydrogen up to $H/Me \approx 1.32$, whereas, at $0.6 \le x \le 1$, the achieved maximum practically did not change. Comparative investigations were also carried out at pressures in the range of 7–30 MPa and at two temperatures, 80 and 293 K, but the amount of absorbed hydrogen H/Me did not exceed ≈1.32.

The results of Refs. [77, 99] on the effect of zirconium additions on the hydrogen absorption properties of alloys based on $TiMn_2$ intermetallic compound were obtained exclusively on the alloys with the stoichiometric composition of the AB_2 phase. However, the question of how the deviation from stoichiometry will affect the sorption–desorption kinetics and the amount of absorbed hydrogen in the alloys of the Ti–Zr–Mn system with AB_2-type structure remained important. The effect of deviation from stoichiometry on the hydrogen absorption properties of $(Ti_{0.95}Zr_{0.05})Mn_{2-x}$ alloys (where $x = -0.05$, 0, 0.05, 0.15, 0.35) was investigated in Ref. [76]. Regardless of the selected chemical composition, all the alloys in the studied range were single-phase and comprised of the hexagonal Laves phase of $C14$ type. The process of interaction with hydrogen was investigated at a pressure of 5 MPa and at 150 °C. It was found out that, at manganese concentrations in the range of $-0.05 \le x \le 0.05$, the amount of absorbed hydrogen increased from $H/Me \approx 0.97$ up to 1.02; and on the contrary, further increase in x from 0.05 to 0.35 (reduction of manganese content) led to a decrease in the hydrogen capacity H/Me from 1.02 to 0.88. Nevertheless, the equilibrium plateau of pressure and hysteresis effect decreased with x in the entire range of $-0.05 \le x \le 0.35$. As mentioned above (see Figs. 2 and 3), lowering the pressure plateau significantly accelerates the formation of hydride, and reducing hysteresis enhances the hydrogen desorption.

The decrease in the amount of absorbed hydrogen in the range of $0.05 \le x \le 0.35$, as well as the lowering of the equilibrium pressure plateau and less pronounced hysteresis effect were explained in [76] by the distortion of interstices, in which dissolved hydrogen is located; this coincides with the data of [100, 101].

The idea proposed in [76] that some reduction of manganese content in the $TiMn_2$-based alloys has a positive effect on the amount of absorbed hydrogen was used in Ref. [96] where the powders of $Ti_{1-x}Zr_xMn_{1.4}$ alloys (x = 0, 0.1, 0.2, 0.3, 0.4) were investigated. It is shown that the alloys had single-phase structure (hexagonal Laves phase of $C14$ type) in the whole concentration interval. However, increasing zirconium content led to an increase in the lattice parameters from a = 0.48620 nm and c = 0.79777 nm at x = 0 to a = 0.49837 nm and c = 0.81719 nm

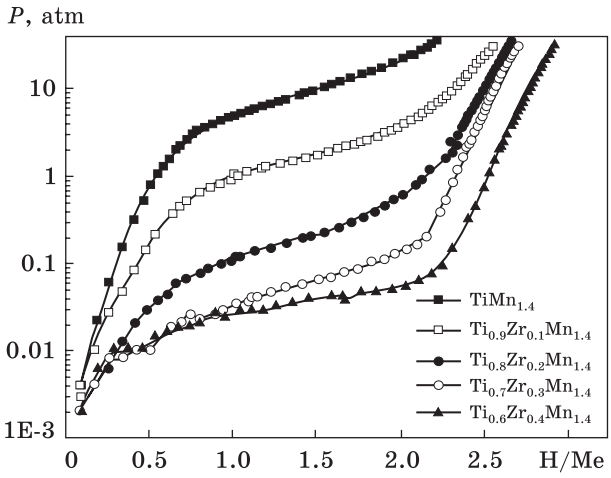

Fig. 13. Pressure–content isotherms of hydrogen sorption in $Ti_{1-x}Zr_xMn_{1.4}$ alloys at 20 °C [96]

at $x = 0.4$, which was explained by the larger atomic radius of zirconium compared to titanium. The interaction of the alloys with hydrogen was investigated at room temperature and a pressure of 3 MPa. The equilibrium pressure plateau lowered at higher zirconium content, whereas the amount of absorbed hydrogen increased (Fig. 13).

For example, for the $TiMn_{1.4}$ alloy ($x = 0$), the amount of absorbed hydrogen was $H/Me \approx 0.92$, whereas, in the $Ti_{0.6}Zr_{0.4}Mn_{1.4}$ alloy ($x = 0.4$), it increased up to $H/Me \approx 1.22$. Based on the literature data [102], the authors of Ref. [96] associated this increase in hydrogen absorption both with larger lattice parameters and, accordingly, with the radius of interstices for hydrogen atoms, and with different affinities of zirconium and titanium to hydrogen. The process of hydrogen desorption was carried out in the same way as in the previous studies [83, 88] by reducing the hydrogen pressure from 3 to 0.01 MPa. For example, in the $TiMn_{1.4}$ ($x = 0$) alloy, the amount of desorbed hydrogen was $H/Me \approx 0.79$, whereas, for the $Ti_{0.9}Zr_{0.41}Mn_{1.4}$ ($x = 0.1$) alloy, it increased to $H/Me \approx 0.91$. On the contrary, a significant decrease was observed at zirconium content $0.1 \le x \le 0.4$: for the $Ti_{0.6}Zr_{0.4}Mn_{1.4}$ alloy ($x = 0.4$), the amount of desorbed hydrogen was only $H/Me \approx 0.35$. The decrease in the amount of desorbed hydrogen with zirconium content was associated in Ref. [96] with greater affinity of zirconium for hydrogen as compared to titanium. Therefore, we can conclude that there are optimal concentrations in the ternary system Ti–Zr–Mn, which provide both high hydrogen absorption and acceptable stability of the hydrogenated material (in other words, acceptable kinetics of hydrogen sorption–desorption under certain thermobaric conditions).

In Ref. [56], based on the data of [76, 96, 99, 103], the simultaneous effect of zirconium additions and deviation from stoichiometry on the hydrogen absorption properties of the alloy based on AB_2 intermetallic phase was investigated on the example of the $(Ti_{0.34}Zr_{0.66})Mn_{1.2}$ alloy. This alloy comprises of the hexagonal Laves phase of $C14$ type. Based on the data on the phase composition of the alloy, the authors noted

that, due to the partial replacement of titanium with zirconium, it was possible to expand the range of the Laves phase to 54.4 at.% Mn (for the binary $TiMn_2$, limit is of 59 at.% [87]) and to get somewhat larger lattice parameters, which is promising for increasing the hydrogen capacity. According to [84–86], the lattice parameters in binary $TiMn_2$ intermetallide were $a = 0.4812–0.4880$ nm and $c = 0.7892–0.7992$ nm, whereas, the lattice parameters in the $(Ti_{0.1}Zr_{0.9})Mn_2$ alloy were $a = 0.5029$ nm and $c = 0.8265$ nm [104], and in the $(Ti_{0.34}Zr_{0.66})Mn_{1.2}$ alloy, $a = 0.5051$ nm and $c = 0.8297$ nm [56].

The interaction of the $(Ti_{0.34}Zr_{0.66})Mn_{1.2}$ alloy with hydrogen was studied at room temperature and hydrogen pressure of 0.6 MPa in as-cast bulk condition. It was found that the incubation period (time from contact of the sample with hydrogen to the start of active interaction) was only a few minutes, and the process of interaction with hydrogen occurred at high rates; it is possible to achieve the amount of absorbed hydrogen $H/Me \approx 1.2$ (for the binary $TiMn_2$ compound, $H/Me \approx 1.0$ [83–88]). As noted in [105], the incubation period is caused by the oxide scale, which is always present on the surface of titanium and Ti-based alloys and is a barrier to the penetration of hydrogen into the bulk. Basing on the data of Refs. [106, 107], the author of Ref. [105] unexpectedly claims that the oxide scale with a thickness of less than 0.45 μm can even be useful, promoting the dissociation of hydrogen molecules into atoms and, accordingly, enhancing the interaction with hydrogen. However, the interaction process is significantly slowed down usually at an oxide scale thickness of 0.5–1.0 μm, and at a thickness of more than 1.0 μm, it stops altogether [108]. Typically, vacuum annealing above 600 °C is applied to activate the interaction of titanium with hydrogen, because at these temperatures, the surface oxide layer dissolves, and the barrier disappears, which leads to the instantaneous onset of metal interaction with hydrogen.

The hydrogen desorption was carried out, as in Refs. [83, 88], by means of reducing hydrogen pressure from 0.6 to 0.002 MPa; as the authors noted, it allowed to reduce the amount of absorbed hydrogen H/Me from 1.2 to 1.0. Desorption of all absorbed hydrogen in the $(Ti_{0.34}Zr_{0.66})Mn_{1.2}$ alloy required heating at an initial pressure of $4 \cdot 10^{-3}$ Pa to 350 °C, whereas, in Ref. [88], it was shown that for binary $TiMn_2$ intermetallide, this temperature was 400 °C, and there was a need to apply 60-minute exposure.

The differences in the parameters of hydrogenation (reduction of hydrogen pressure from 3.2 MPa [83] to 0.6 MPa) and dehydrogenation (drop of the temperature of complete dehydrogenation from 400 °C [88] to 350 °C), as well as the increase in the amount of absorbed hydrogen to $H/Me \approx 1.2$, were explained in Ref. [56] by the following factors. First, it is reduction of the minimum manganese content needed for the

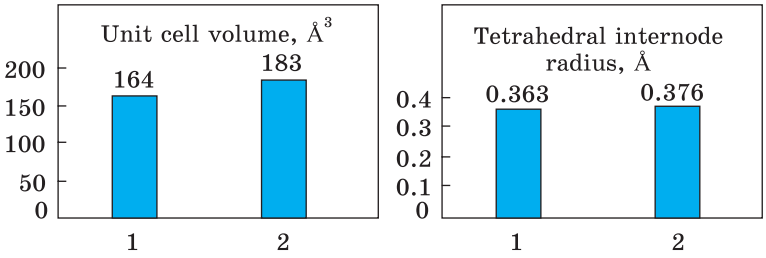

Fig. 14. Unit cell volume and tetrahedral interstice radius of Laves phase of *C*14 type in $TiMn_2$ (*1*) [83] and $(Ti_{0.34}Zr_{0.66})Mn_{1.2}$ (*2*) [56] alloys

Laves phase stabilization [83, 88]. Second, it is a significant increase of the unit cell volume and the radius of the tetrahedral interstice in the $(Ti_{0.34}Zr_{0.66})Mn_{1.2}$ alloy as compared to the binary $TiMn_2$ compound (Fig. 14). The radius of the tetrahedral interstice was calculated from the hard spheres approximation by formula $R_{s(C14)} = 0.074475a$, where a is the lattice parameter taken from the literature [109, 110].

The data in Fig. 14 confirm the assumptions made in [2, 30, 93–96] that partial replacement of titanium with zirconium leads to an increase in the lattice parameter, and therefore, increases the radius of interstices, which enhances the total amount of absorbed hydrogen.

In the above-mentioned works, the positive effect of alloying and deviation from the stoichiometric composition AB_2 on the hydrogen absorption properties of the alloys based on intermetallic AB_2 compound was proved. However, the investigations were performed only for a partial replacement of titanium with zirconium (the component *A*). In Refs. [74, 111–113], the authors proposed to determine the effect of partial replacement of component *B* (*i.e.*, to substitute manganese that does not interact with hydrogen for vanadium that is able to interact with hydrogen) in the intermetallic AB_2-based alloys.

This idea was developed in Ref. [111]; the simultaneous effect of partial substitution of component *A* (titanium for zirconium) and component *B* (manganese for vanadium) on the hydrogen absorption properties of AB_2 intermetallides was studied on the example of $(Ti_{0.9}Zr_{0.1})(Mn_xV_y)$ alloys, where $x = 1.1–2.2$ and $y = 0.1–0.7$. Referring to the literature [83], the authors of Refs. [74, 111] noted that the binary intermetallic $TiMn_2$ compound can contain up to 25 at.% V without affecting the phase composition, which allows to expand the homogeneity of the intermetallic phase to 38–63 at.% Mn (for binary intermetallics, the concentration limits are of 59–70 at.% Mn [83]). It was shown in [85] that the simultaneous introduction of two elements (zirconium and vanadium) in the $TiMn_2$ allowed to increase vanadium content up to 26 at.% V and, thereby, to expand the homogeneity region to 36–65 at.%

Mn. The interaction of $(Ti_{0.9}Zr_{0.1})(Mn_xV_y)$ alloys with hydrogen was investigated at 20–100 °C and hydrogen pressure of 1 MPa. It was noted that for activation these alloys require preliminary long-term exposure at 850–900 °C for 240 hours. It was determined that after such treatment the interaction with hydrogen occurred at a fairly high rate that allowed to achieve the amount of absorbed hydrogen at the level of 1.8–2.0 wt.% that corresponds to the composition $H/Me \approx 1.0–1.2$. The amount of absorbed hydrogen was slightly higher than for the binary $TiMn_2$ intermetallics ($H/Me \approx 1.0$ [83]), but the material did not exceed the performance of alloys whose hydrogen absorption properties were studied in [96, 99].

As shown in Refs. [56, 74, 76, 96], the partial substitution of elements *A* and/or *B* for zirconium and vanadium in the binary $TiMn_2$ compound allowed to expand the region of its homogeneity to 36–65 at.% Mn (for $TiMn_2$, it is 59–70 at.% Mn [83]). An explanation of this fact was given in [111], based on the data previously presented in [112]. The authors of Ref. [111] experimentally proved that under the lack of component *B* (less than needed for stoichiometric AB_2 composition) some atoms of component *A* (for these alloys it is titanium, because the size of its atom is closer to manganese) shift to unfilled positions of component *B* (manganese), and as a result, it is possible to obtain stoichiometry AB_2.

As shown above, the introduction of zirconium and/or vanadium into the binary $TiMn_2$ compound led to an increase in the amount of hydrogen absorbed and affected in some way the kinetics of the sorption-desorption processes. As noted in the above-mentioned works, the improvement of properties occurred due to the differences in atomic radii (atomic radius of titanium is of 0.147 nm, and for zirconium, is of 0.160 nm), as well as in hydrogen activity (unlike manganese, vanadium is a hydride-forming element).

The investigations of the effect of alloying on the hydrogen absorption properties of the $TiMn_2$-based alloys were extended in Refs. [114, 115] on the example of the $(Ti_{0.34}Zr_{0.66})Mn_{0.96}V_{0.12}Cr_{0.11}$ alloy. The authors proposed the simultaneous partial substitution of component *B* for two elements, which interact with hydrogen. Based on the literature data [116], the authors of Refs. [114, 115] chose chromium which can effectively influence the kinetics of both sorption and desorption of hydrogen, as well as the hydrogen capacity of the $TiMn_2$-based alloys. The authors of Refs. [114, 115] noted that in contrast to the previously considered alloys, the studied $(Ti_{0.34}Zr_{0.66})Mn_{0.96}V_{0.12}Cr_{0.11}$ alloy consisted of two phases: hexagonal Laves phase of *C*14 type, and cubic phase of *C*15 type. The authors explained the appearance of the second intermetallic phase by the fact that there is the Laves phase of *C*15 type in binary zirconium–chromium and titanium–chromium systems at room temperature (see Refs. [117, 118]).

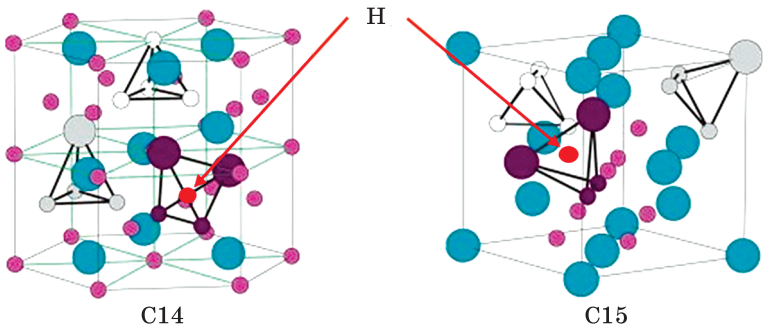

Fig. 15. Unit cell of AB_2-type intermetallics, where larger (smaller) balls correspond to *A* (*B*) component [110]

The interaction of the $(Ti_{0.34}Zr_{0.66})Mn_{0.96}V_{0.12}Cr_{0.11}$ alloy with hydrogen was investigated at room temperature and hydrogen pressure of 0.23 MPa on bulk samples without preliminary heat treatment. Under these conditions, the active absorption of hydrogen by the alloy during the first hydrogenation started after an incubation period of 2–10 minutes and lasted about 10 minutes; the hydrogen capacity was $H/Me \approx 1.36$ that is significantly higher as compared to the binary $TiMn_2$ compound ($H/Me \approx 1.0$ [83, 88]).

The hydrated $(Ti_{0.34}Zr_{0.66})Mn_{0.96}V_{0.12}Cr_{0.11}$ alloy started to release hydrogen at an initial pressure of $4 \cdot 10^{-3}$ Pa at room temperature, but it was possible to remove no more than 4% of the absorbed hydrogen in these conditions. Heating was necessary to resume the hydrogen desorption from the mixture of hydrides: the maximum desorption rate was observed at 115 ± 5 °C, and at 300 °C, all hydrogen was desorbed. The authors of Refs. [114, 115] explained some decrease in the temperature of complete hydrogen desorption as compared, for example, to the $(Ti_{0.34}Zr_{0.66})Mn_{1.2}$ alloy [56] and the binary $TiMn_2$ compound [83, 88], by the presence of the Laves phase of *C*15 type, which has both types of interstices: tetrahedral and octahedral.

This explanation was drawn in Refs. [114, 115] from the analysis of literature data [119, 120], according to which, the decrease in thermal stability of the hydrides based on intermetallics of AB_2 type (Laves phase) is caused by partial substitution of *A* or *B* atoms by other elements due to electron or chemical effects [121, 122]. The authors of Refs. [114, 115] suggested that hydrogen atoms in the Laves phase of *C*15 type with f.c.c. lattice are located in the octahedral interstices, because these interstices are almost twice as large as tetrahedral; this reduces the thermal stability of the hydride based on the $(Ti_{0.34}Zr_{0.66})Mn_{0.96}V_{0.12}Cr_{0.11}$ alloy. However, in Ref. [110], it was proved that, regardless of the type of crystal lattice of the Laves phase (h.c.p. or f.c.c. one), hydrogen is located exclusively in the tetrahedral interstices (Fig. 15).

Thus, the authors of [110] provided data that the hydride obtained by them on the basis of the *C*15-type Laves phase had a lower thermal stability than that based on *C*14-type phase. The authors explain this difference by geometric factors (the change of lattice from h.c.p. to f.c.c. one), accompanied by the decrease in the number of atoms per unit cell (from 12 atoms in h.c.p. lattice to 6 in f.c.c. lattice), and the reduction of the radius of tetrahedral interstices where dissolved hydrogen atoms are located.

Based on the previous studies [74, 111–115, 123], the investigations of the simultaneous effect of partial replacement of components *A* and *B*, as well as deviations in the concentration of elements from the stoichiometric AB_2 composition, were continued in Ref. [124]. In contrast to the previous studies, the deviation of stoichiometry was not due to a decrease in the amount of component *B* (manganese), but due to increased amount of *A* (titanium and zirconium); besides, four elements already played the role of component *B*. Therefore, the authors of Ref. [124] described the chemical composition of the alloys studied by the following formula: $(Ti_{0.85}Zr_{0.15})_{1.05}Mn_{1.2}Cr_{0.6}V_{0.1}Me_{0.1}$ (where *Me* = Ni, Fe, Cu). The authors experimentally proved that the three alloys studied (separately with nickel, cobalt and copper) were single-phase with the structure of the hexagonal *C*14-type Laves phase but these alloys had slightly different lattice parameters. For example, in the $(Ti_{0.85}Zr_{0.15})_{1.05}Mn_{1.2}Cr_{0.6}V_{0.1}Ni_{0.1}$ alloy, the lattice parameters were a = 0.48937 nm and c = 0.80324 nm, so, they were larger than for the binary $TiMn_2$ compound (a = 0.4812–0.4880 nm, c = 0.7892–0.7992 nm [84–86]). The authors noted that the addition of alloying components in the sequence Ni–Fe–Cu led to a gradual increase of the lattice parameters, and accordingly larger radius of the tetrahedral interstice [92], *i.e.*, favourable for enhanced hydrogen capacity. For example, after substitution of Ni for Fe, the parameters increased to a = 0.48940 nm and c = 0.80331 nm, and after using copper, they were a = 0.48954 nm and c = 0.80353 nm, and the unit cell volume increased from 165.591 to 166.771 Å^3, respectively. The increase of the lattice parameters and, accordingly, the volume of the unit cell caused by the transition from nickel to copper, was explained in Ref. [124] basing on the data of Ref. [125] by the different atomic radii of these elements (0.125 nm and 0.128 nm, respectively), as the content of all other components was constant.

The interaction of the Ni-, Fe-, and Cu-containing alloys with hydrogen was carried out in Ref. [124] at room temperature and hydrogen pressure of 4 MPa. The authors noted that there was required an activation sorption–desorption cycle in these alloys to achieve the high amount of absorbed hydrogen and the rate of interaction. The highest amount of absorbed hydrogen in alloys containing Ni, Fe, and Cu equalled 1.79–1.81 wt.%. The increase in the content of absorbed hydrogen upon the

transition from nickel to copper as alloying element the authors associated with different lattice parameters. The authors noted that they achieved somewhat higher concentration of absorbed H as compared, *e.g.*, to $(Ti_{0.85}Zr_{0.15})_{1.1}Cr_{0.925}MnFe_{0.075}$ alloy used in high-pressure tanks [126] (reference alloy), despite the larger number of alloying components, comparable with $(Ti_{0.9}Zr_{0.1})(Mn_xV_y)$ alloys considered in Ref. [74].

Therefore, summarizing the results of the above-mentioned works on the study of the effect of alloying on the hydrogen absorption properties in the binary $TiMn_2$ intermetallics, it is clearly seen that the transition from the binary Ti–Mn system to more complex systems, including up to 6 components, allowed to increase the amount of absorbed hydrogen H/*Me* from 1.0 to 1.36, but in some cases the sorption-desorption kinetics were significantly deteriorated.

Therefore, some researchers suggested more integrated approach with aim to achieve a more significant increase in the amount of absorbed hydrogen and, most importantly, not to lose the positive parameters of the sorption–desorption kinetics in the alloys based on AB_2-type intermetallics [127–131]. The idea is to deviate from the stoichiometric AB_2 composition with simultaneous alloying and changing the general phase and structural state of the material. Thus, it was proposed to use another factor affecting the hydrogen capacity as shown in Fig. 11, namely, the phase composition.

5. Effect of Phase and Structural Changes on Hydrogen Absorption Properties of $TiMn_2$ Intermetallics

The authors of Refs. [127, 128] studied the hydrogen adsorption properties of the alloys of Ti–V–Mn and Ti–Zr–Mn–V systems based on the AB_2-type intermetallics and experimentally found out the second phase, along with the Laves phase. Later, this phase was identified as the b.c.c. Ti-based solid solution. Using the Rietveld method, the authors [127, 128] determined the volume fractions of two phases: 85 and 15% (in some cases even more) of AB_2-type intermetallics and the b.c.c. solid solution, respectively. Figure 16 shows a typical microstructure for this class of materials, where the dark areas correspond to the Laves phase, and the light ones, to the b.c.c. solid solution.

B.c.c. titanium-based solid solutions have rather high (4 wt.%) hydrogen capacity [30] compared to the intermetallics. However, titanium alloys with b.c.c. lattice have never been considered as commercial materials for hydrogen storage [132–134] because of the need for their technologically complex preliminary thermal activation, low hydrogenation rate even at so high temperatures as 400–600 °C, and high temperature range of desorption (Table 3). Therefore, it has long been believed [135–138] that the presence of even a small amount of the b.c.c.

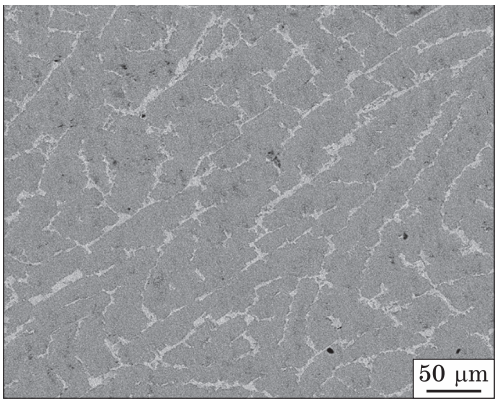

Fig. 16. Typical microstructure for two-phase Laves-phase-based alloys [131]

phase in the alloys based on the AB_2-type intermetallics would deteriorate their hydrogen sorption–desorption kinetics. However, an interesting fact was found out in Refs. [127, 128]: there were no inflections or steps on the dependences of pressure on the amount of hydrogen absorbed by the material (pressure–concentration diagrams) plotted for the hydrogenation process. This indicates that the process of hydrogen sorption is single-stage, *i.e.*, two-phase alloys interact with hydrogen as single-phase ones. In Refs. [129–131], a one-stage process of hydrogen sorption was also observed in the alloys with a volume fraction of b.c.c. solid solution up to 35%. Thus, it was proved that the b.c.c. solid solution in combination with AB_2 phase could interact with hydrogen under the thermobaric conditions needed for the hydrogenation of intermetallics.

In Refs. [127–131], it was shown varying the ratio between the AB_2 and b.c.c. phases in the two-phase alloys allowed to change the amount of absorbed hydrogen in a wide range. Besides, an important fact for practical use was found out: the kinetics of both sorption and desorption of hydrogen in the two-phase alloys remained the same as for single-phase alloys comprised only of the AB_2-type intermetallic phase. Based on this, the authors of Refs. [127, 128] proposed a new concept for developing materials with high hydrogen capacity, namely, 'Laves phase-related b.c.c. solid solution'.

The mechanism of hydrogenation of the b.c.c. solid solution at room temperature and at high rates was experimentally clarified on the example of $Ti_{42.75}Zr_{27}Mn_{20.25}V_{10}$ alloy in Ref. [139]. The authors showed that the facilitated interaction of b.c.c. Ti-based solid solution with hydrogen in the presence of the Laves phase occurred at room temperature with high rates similar to the kinetics of hydrogen sorption by intermetallic due to the following factors. Firstly, there is no need to create special conditions on the surface of the b.c.c. solid solution for facilitated dissociation of hydrogen molecule into atoms, because the dissociation occurs rapidly on the surface of intermetallic crystallites. Secondly, the cast alloy (as a bulk material) has the highest density of contact between the phases, which facilitates the diffusion of hydrogen through the interphase boundaries. Finally, after the start of the hydrogenation process,

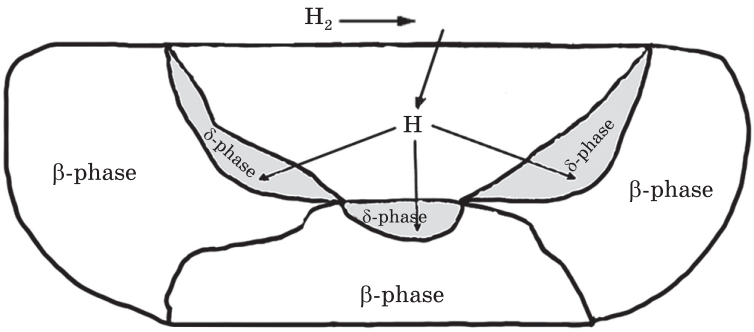

Fig. 17. Schematic diagram of hydride formation in two-phase alloys [139]

the cracking of the surface of intermetallic crystallites increases the surface area for absorption and faster hydrogen penetration into the material volume. According to the above mentioned, the authors of [139] proposed a schematic diagram of hydride formation for these two-phase materials, based on the example of the alloy studied (see Fig. 17).

According to Refs. [127, 128], the positive effect of a certain amount of b.c.c. solid solution in the AB_2-based alloys on the amount of absorbed hydrogen was found out, and this was used in Ref. [140] to develop new alloys for hydrogen storage. The authors investigated $Ti_xV_{35}Mn_{65-x}$ alloys (where x = 20, 25, 30, 35, 40 at.%) which, in contrast to those studied in Refs. [127, 128], should have had a much larger volume fraction of b.c.c. solid solution [141, 142]. As has been expected, all alloys were two-phase and comprised of b.c.c. solid solution and intermetallic AB_2 phase. According to Ref. [140], higher content of titanium in this range leads to increased volume fraction of b.c.c. solid solution and titanium content in it, as well as larger lattice parameters, that correlates well with the data of [143, 144].

The interaction of the $Ti_xV_{35}Mn_{65-x}$ alloys (x = 20, 25, 30, 35, 40 at.%) with hydrogen was investigated at room temperature and hydrogen pressure of 4 MPa. The authors noted that these alloys require rather complex preliminary activation, as well as at least three activation cycles of hydrogen sorption–desorption to achieve the highest possible hydrogen capacity and the ability to interact with hydrogen at room temperature at a high rate. The increase in x in this range leads to a significant higher absorption of hydrogen. For example, at x = 20, the amount of absorbed hydrogen was 2.63 wt.% (H/$Me \approx 1.4$), whereas, at x = 35, it was 3.35 wt.% (H/M$e \approx 1.76$), but this significantly worsened the kinetics of hydrogen desorption. The increase in the total amount of absorbed hydrogen, in comparison with the single-phase AB_2 state, was explained (in Ref. [140] according to [145]) by the higher volume frac-

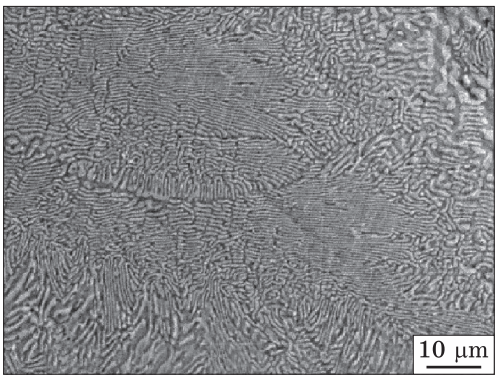

Fig. 18. Typical microstructure of eutectic alloy [146]

tion of b.c.c. solid solution and titanium content in it.

The hydrogen desorption was studied under the hydrogen pressure reduced from 4 to 0.002 MPa. In these conditions, only a part of the accumulated hydrogen was removed: 0.93 wt.% (H/*Me* ≈ ≈ 0.49) at x = 20, and 1.18 wt.% (H/*Me* ≈ 0.6) at x = 35, and the authors emphasized that the desorption of all absorbed hydrogen required rather stringent thermobaric conditions.

Comparing the data on the interaction of two-phase alloys comprised of b.c.c. solid solution and AB_2-phase with hydrogen, one can draw an important conclusion. The use of multiphase alloys makes it possible to replace effectively single-phase intermetallics as hydrogen sorbents due to the possibility to obtain much higher amounts of absorbed hydrogen, but it is important to preserve the kinetic parameters of fast sorption–desorption, which are characteristic for the single-phase alloys of AB_2-type.

Based on the previous studies [127, 128], a new approach to the development of AB_2 + b.c.c. solid solution materials for H sorption were proposed in Refs. [146–152]. The authors proposed to use the eutectic alloys (natural composites) comprised of AB_2-type intermetallics (Laves phase) and b.c.c. Ti-based solid solution (Fig. 18).

By the example of the eutectic $Ti_{47.5}Zr_{30}Mn_{22.5}$ alloy, the authors of Ref. [146] showed that the eutectic solidification of this material automatically provided the condition of the minimum possible manganese content in the AB_2-type intermetallide (the need for the lowest possible manganese content in the $TiMn_2$-based alloys was proved in Ref. [83]), and there was a net of interphase boundaries with a high specific surface area (Fig. 18). This should contribute to fast kinetics of hydrogen absorption; as it is known from the literature [153], a high rate of hydrogen penetration into the material volume is provided, in particular, by its diffusion along the grain boundaries. In addition, the eutectic solidification of this alloy allows stabilizing the Ti-based b.c.c. solid solution at room temperature, which is important for the interaction with hydrogen. The hydrogen capacity of the titanium-based β-phase is of 4 wt.% [30], while for the α-phase, it is only 0.01 wt.% [154, 155], and the diffusion coefficient of hydrogen in the β-phase is 3.5 times higher than in the α-phase [156].

The hydrogen absorption properties of the $Ti_{47.5}Zr_{30}Mn_{22.5}$ alloy were studied at room temperature and hydrogen pressure of 0.6 MPa. The alloy interacted with hydrogen in these conditions at high rate, but an activation heating was required during the first hydrogenation up to 520 °C at the applied pressure for subsequent hydrogen desorption [146]. The amount of absorbed hydrogen was 2.58 wt.% (62.6 at.% H), which corresponded to the formula composition $H/Me \approx 1.64$, whereas the hydrogen capacity of the AB_2-type alloys did not exceed 2.1 wt.% ($H/Me \approx 1.36$) [114, 115]. However, it should be noted that the desorption of all absorbed hydrogen could be achieved only by heating to 550 °C, while, for AB_2-based alloys, heating up to 350–400 °C was needed [56, 88]. The authors of Ref. [146] explained the increase in the temperature (needed for complete H desorption) by the presence of more stable hydride phase based on the b.c.c. solid solution. According to Ref. [52], the decomposition of the hydride based on titanium or b.c.c. solid solution occurs at 300–600 °C.

The study of eutectic alloys of the Ti–Zr–Mn system with the structure of AB_2 and b.c.c. solid solution was extended in Ref. [147], and the effect of changes in the initial structure (ratio of phase volume fractions) on the hydrogen absorption kinetics and the amount of hydrogen absorbed during the first hydrogenation was shown.

The authors investigated the $Ti_{80-x}Zr_{20}Mn_x$ alloys with x = 21.5, 25, 28.5 at.%; this allowed to study the full range of the alloys from pre-eutectic (primary crystallites of b.c.c. solid solution) to hypereutectic (primary crystallites of intermetallic AB_2 phase). As for the $Ti_{47.5}Zr_{30}Mn_{22.5}$ alloy [146], the interaction with hydrogen was studied at room temperature and hydrogen pressure of 0.6 MPa, and these alloys also required the first sorption–desorption cycle to activate the reaction with hydrogen at room temperature and the mentioned pressure at high rate.

The authors of Ref. [147] noted that the first sorption–desorption cycle led to the transition of a bulk sample to a powder state, which enhanced the reaction surface for dissociation of hydrogen molecules, activated the invasion of hydrogen into the bulk material, and improved the interaction kinetics. It is important that due to the different initial structures, and accordingly, different ratio of the volume fractions of phases, it was possible to get the amount of absorbed hydrogen in rather wide range from 2.81 wt.% (pre-eutectic composition) to 2.49 wt.% (eutectic composition), which corresponded to the formula composition H/Me from 1.67 to 1.49, respectively.

Rather significant difference in the amount of absorbed hydrogen was associated in Ref. [147] with the different titanium/manganese ratios, as well as with significantly different hydrogen capacities of intermetallic AB_2 phase (2 wt.% [74]) and the b.c.c. Ti-based solid solution (4 wt.% [30]).

The mentioned above data on the interaction of eutectic alloys comprised of intermetallic AB_2-type phase and b.c.c. solid solution with hydrogen show that variations in chemical composition allow to obtain different initial structures and, accordingly, different ratios of volume fractions of two phases; this allows to change the hydrogen capacity in rather wide range without significantly changes in the kinetics of hydrogen sorption. The investigated eutectic alloys, as well as the alloys based on the intermetallic AB_2 compound, require the first activation cycle for efficient and fast interaction with hydrogen at room temperature. The hydrogen absorption properties of eutectic alloys and two-phase alloys based on intermetallics can be enhanced by means of another factor that affects the hydrogen capacity, namely, preliminary heat treatment (see the scheme in Fig. 11).

6. Influence of Preliminary Heat Treatment on the Kinetics of Interaction with Hydrogen for Multiphase Alloys

As known from the literature [157, 158], the preliminary heat treatment (annealing) of multiphase alloys is an effective way to affect chemical composition of phases, the size of individual crystallites, the volume fractions of phases and the catalytic properties of the interphase boundaries. The obtained data on the positive effect of changes in the chemical composition of the phases [76, 96] or the volume fractions of phases [127, 128] on the kinetic parameters of sorption–desorption and the amount of absorbed hydrogen were used in Refs. [159–162] to determine the effect of preliminary heat treatment on the properties of two-phase alloys comprised of b.c.c. solid solution and Laves phase. However, the results presented in the literature, especially in [161, 162], on the effect of heat treatment on the hydrogen absorption properties of multiphase alloys are varying due to variations in chemical composition, processing routes and experimental conditions, that does not allow unambiguous interpretation of these data.

For example, various heat treatments were tested on the multiphase $Ti_{10}V_{77}Cr_6Fe_6Zr$ alloy in Ref. [161]. Annealing at 1100 °C for 8 hours or heating to 1250 °C for 5 minutes were followed by water quenching. The alloy in as-cast condition and after various heat treatments had two-phase structure comprised of b.c.c. solid solution and Laves phase. This indicates that no new phases appeared in the alloy upon heat treatment, but according to the authors [161], the volume fractions of two phases changed (the amount of b.c.c. solid solution increased). The higher volume fraction of b.c.c. solid solution made possible to increase the amount of absorbed hydrogen, but, at the same time, the kinetics of interaction with hydrogen deteriorated (the rate of hydrogen absorption decreased).

Besides, it was noted that, after heat treatment at 1250 °C and 5-min exposure, hydrogen desorption rate enhanced as compared to the alloy in as-cast condition. For example, the as-cast alloy released 1.44 wt.% hydrogen at 60 °C and hydrogen pressure of 0.1 MPa, whereas, after the mentioned heat treatment, it released 1.82 wt.%.

The effect of heat treatment on the hydrogen absorption properties of $V_{35}Ti_{20}Cr_{45}$ alloy was studied in Ref. [162]. The alloy in as-cast condition had single-phase structure (b.c.c. solid solution). Heat treatment (annealing at 700 °C for 72 hours) led to redistribution of chemical elements and the formation of the second phase. The new phase was identified as the Laves phase of *C*14 type. The preliminary heat treatment was shown to enhance the processes of hydrogen sorption–desorption; at the same time, the amount of absorbed hydrogen decreased. The authors attributed the enhancement of the sorption–desorption kinetics and the reduction of the amount of absorbed hydrogen to the formation of the Laves phase. Since the hydrogen capacity of the b.c.c. solid solution is twice higher compared to the Laves phase, the formation of the latter is expected to reduce the total amount of absorbed hydrogen.

As shown above, the results of Refs. [161, 162] are quite different from those obtained in Ref. [163] on the effect of heat treatment of multiphase alloys; therefore, a more comprehensive study of the effect of preliminary heat treatment on the hydrogen absorption properties was undertaken, based on these data.

The authors of Ref. [163] chose for their study a multiphase $Ti_{15.6}Zr_{2.1}V_{40}Cr_{11.2}Mn_{6.9}Co_{1.4}Ni_{22.5}Al_{0.3}$ alloy (it had a higher electrochemical capacity and desorption rate compared to analogues [164]), as it is a dual-purpose alloy, which can be used both in hydrogen storage tanks and in Ni-H*Me* hydride batteries. The alloy in as-cast condition comprised of the b.c.c. solution, the Laves phase of *C*14 type and the intermetallic TiNi phase that coincided with the data of Ref. [165]. In order to confirm the need for heat treatment and determine the optimal regimes of annealing, the temperature range of 800–1100 °C with exposure times 5–12 hours was studied (Fig. 19). As revealed, the heat treatment caused different effects on the phase composition and the volume fractions of the phases. For example, annealing at 800–900 °C led to an increase in the volume fraction of b.c.c. solid solution, whereas the volume fractions of the Laves phase and TiNi intermetallide reduced from 10.5 to 2.8 and from 23.9 to 14.1%, respectively (Fig. 19). On the contrary, increasing the annealing temperature to 1000 °C caused an increase in the volume fraction of the Laves phase from 2.8 to 16.8%, and of TiNi intermetallide from 14.1 to 19.2%, as well as to the formation of new intermetallic Ti_2Ni phase. At 1100 °C, the volume fractions of the Laves phase and TiNi intermetallide again decreased, and intermetallic Ti_2Ni phase is not formed; however, two new phases VNi and ZrO_2 formed (Fig. 19).

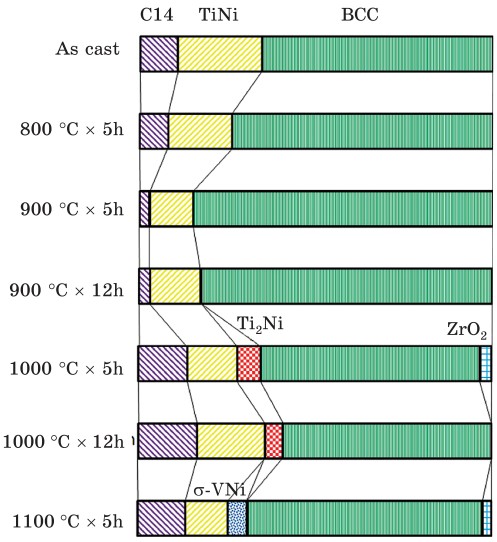

Fig. 19. The phase composition evolution of $Ti_{15.6}Zr_{2.1}V_{40}Cr_{11.2}Mn_{6.9}Co_{1.4}Ni_{22.5}Al_{0.3}$ alloy [163]

This does not contradict the data of Refs. [166, 167].

The interaction of the $Ti_{15.6}Zr_{2.1}V_{40}Cr_{11.2}Mn_{6.9}Co_{1.4}Ni_{22.5}Al_{0.3}$ alloy with hydrogen in different initial states (as-cast, annealed) was investigated at room temperature and hydrogen pressure of 5 MPa. The authors noted that regardless of the initial state, sorption–desorption cycle was required for activation. An important fact to understand the need for the preliminary heat treatment is the amount of absorbed hydrogen. The alloy in as-cast condition absorbed only 1.7 wt.% hydrogen, which corresponded to $H/Me \approx 0.93$. After heat treatment, the amount of absorbed hydrogen, regardless of the different regimes of heat treatment and changes in the volume fractions of phases, significantly reduced to the level of 1.36 wt.% ($H/Me \cong 0.74$). This reduction in the amount of absorbed hydrogen is unexpected, because the increase in the volume fraction of b.c.c. solid solution, on the contrary, should lead to a noticeable increase in the total hydrogen capacity of the material. The authors of [163] attributed the decrease in the amount of absorbed hydrogen after heat treatment to the changes in the chemical composition of the phases (formation of overstoichiometry [168] when some atoms of the *B* component occupy positions of the *A* component), redistribution of hydrogen-active components between phases [169, 170], and decrease of lattice parameters in all phases. The plateau of hydrogen pressure after annealing at 800–900 °C decreased, whereas after annealing at 900–1100 °C, it increased. The authors explained this by the different volume fraction of b.c.c. solid solution in the alloy, compared to the initial, after various heat treatments, as the hydride based on this phase is more stable than the hydrides formed in the Laves phase and TiNi intermetallide and has the lowest pressure plateau. It was also found out that the hysteresis after heat treatment was more pronounced, which adversely affected the hydrogen desorption.

Therefore, summarizing all the above, it is clear that the preliminary heat treatment of multiphase alloys is an effective method of influencing the amount of hydrogen absorbed and the sorption–desorption kinetics.

As shown above, a combined approach to the development of hydrogen battery materials is an effective way to increase the total amount of

absorbed hydrogen. Thus, it was decided to apply another factor influencing the hydrogen capacity, according to the scheme shown in Fig. 11, namely, to change the method of alloy fabrication.

7. Alloy Production Method

According to the literature [171], today most researchers use the casting method to fabricate alloys for hydrogen batteries. However, the authors of Ref. [171] note that in the case of traditional methods, such as induction or arc melting, segregation inevitably occurs during cooling of the ingot, and this may adversely affect the sorption–desorption kinetics and the amount of absorbed hydrogen. More modern methods of fabricating alloys, based on hardening from melt with a high cooling rate or involving powder technologies, including melt spraying or mechanical alloying, allow to obtain ingots and powders with higher chemical homogeneity and smaller grain size as compared to those produced by traditional casting methods. At the same time, the alloys produced by powder methods usually contain noticeable amount of impurities, which can also significantly affect the hydrogen absorption characteristics. Accordingly, the hydrogen absorption properties of alloys with the same chemical composition, but produced by different methods, can differ significantly.

A comparison of the hydrogen absorption characteristics of powders of an alloy comprised of the Laves phase and produced by spraying in gas and casting with subsequent grinding was made in Ref. [172]. The authors showed that the morphology of particles depended on the parameters of their manufacture and processing methods. The powders produced by mechanical grinding of the ingot had a different shape, while the gas-sprayed powders were spherical. In the study of the hydrogen absorption properties for gas-sprayed particles in comparison with those produced by casting followed by grinding, it was shown that, for particles finer than 50 μm, the amount of absorbed hydrogen significantly dropped, and the hysteresis loop became larger. Besides, the increase in jet pressure of spraying gas led to a reduction in the amount of absorbed hydrogen, and the slope of the plateau pressure significantly increased due to phase separation inside the grains of the gas-sprayed alloy, as well as the conditions on the particle surfaces (gas-sprayed particles had solid hardened and partially oxidized surfaces). The enhancement of hydrogen desorption for the gas-sprayed alloy, compared to the alloy obtained by casting, was mainly caused by the higher pressure at the plateau due to finer grain size and higher energy needed for dissolving hydrogen in interstices in the gas-sprayed state.

A comparative study of the effect of different methods of alloy production (induction melting and mechanical alloying) on the hydrogen

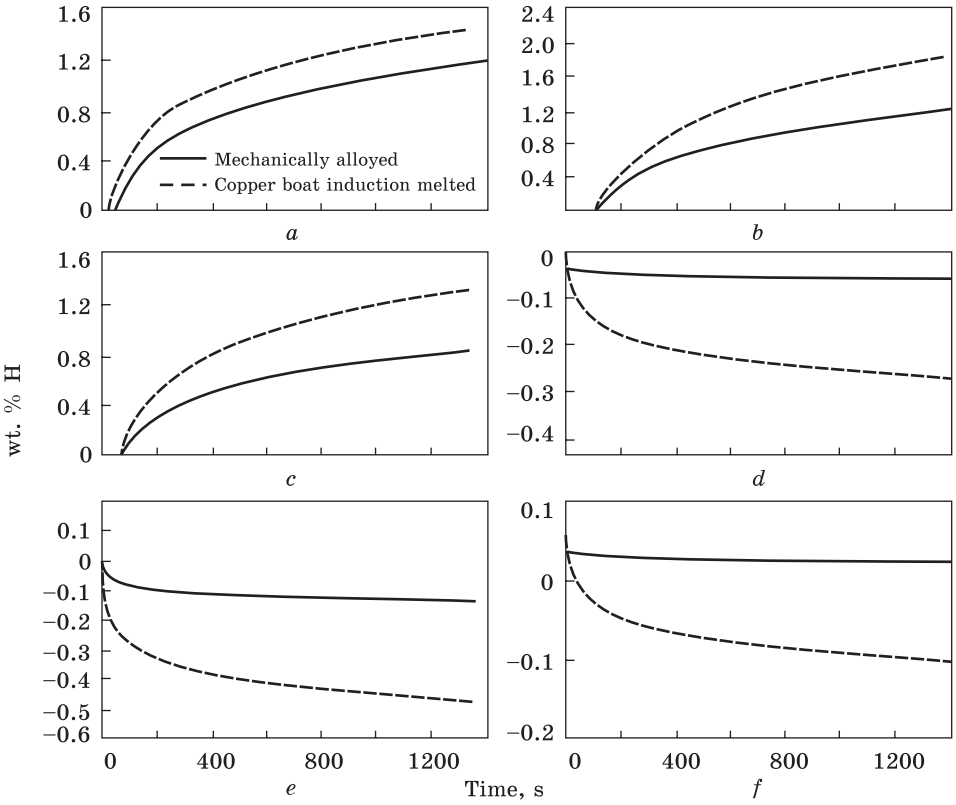

Fig. 20. Absorption (*a*, *b*, *c*) and desorption (*d*, *e*, *f*) curves of $Ti_{0.72}Zr_{0.28}Mn_{1.6}V_{0.4}$ alloy (produced by ball milling and induction melting) at room temperature (*a*, *d*), 150 °C (*b*, *e*), and 400 °C (*e*, *f*) [173]

absorption properties was carried out in Ref. [173] on the example of $Ti_{0.72}Zr_{0.28}Mn_{1.6}V_{0.4}$ alloy. Regardless of the method of production, the alloy comprised of two phases: Laves phase of *C*14 type and b.c.c. solid solution. However, the authors noted that in the alloy produced by induction melting the amount of b.c.c. solid solution was somewhat higher, which was attributed to a high cooling rate in this method. In addition, after induction melting, the elements were distributed in the phases much more homogeneously, which correlates with the data of Ref. [174]. As mentioned, high inhomogeneity in the chemical composition of the phases can significantly affect the amount of absorbed hydrogen. The hydrogenation was carried out at 20, 150, and 400 °C (Fig. 20).

The authors claim that the best thermodynamic and kinetic parameters of the hydrogenation were obtained at 150 °C; the amount of hydrogen absorbed by cast alloy was 2 wt.%, whereas after mechanical alloying, it was only 1.2 wt.%. Besides, the amount of absorbed hydro-

gen after casting was somewhat higher than for alloys comprised only of the Laves phase of *C*14 type [175, 176]. The authors of Ref. [174] attributed the significant difference in the amount of absorbed H after casting and mechanical alloying to several factors: (i) different volume fractions of b.c.c. solid solution; (ii) higher content of impurities (Fe and O) in the alloy after mechanical alloying.

In contrast to the above work, in Ref. [177], it was shown that changing the method of material production could significantly increase the hydrogen capacity and improve the kinetics of hydrogen sorption–desorption. Having compared the hydrogen absorption properties of $V_{35}(Ti,Cr)_{51}(Zr,Mn)_{14}$ alloy fabricated by sintering in plasma spark discharge (spark plasma sintering (SPS) method) and by induction melting, the authors noted that the kinetic parameters of the hydrogenation were the same (hydrogenation temperature 400 °C and hydrogen pressure 2.1 MPa, incubation period of up to 200 seconds), but the amounts of absorbed hydrogen significantly differed. In the SPS alloy, the amount of absorbed hydrogen was 2.89 wt.% which was approximately 24% higher than for the cast alloy (2.32 wt.%). In addition, it was shown that the amount of desorbed hydrogen for the SPS alloy under the same conditions (at 303 K) was 60%, whereas for the cast alloy, it was only 34%. The authors explain such significant differences in both the amount of absorbed and desorbed hydrogen by the fact that there was no diffusion of elements that form the Laves phase (in this case, it was manganese, which does not interact with hydrogen and has a much smaller atomic radius) into the b.c.c. solid solution in the SPS material. Based on the literature data [178], the authors of Ref. [177] claim that the adding manganese in the b.c.c. Ti-based solid solution reduces the lattice parameter and, accordingly, lowers amount of absorbed hydrogen.

Therefore, given all the above regarding the impact of different methods of alloy production on the hydrogen absorption properties, one can conclude that in most cases the transition from traditional casting to other techniques mentioned above deteriorates the sorption–desorption kinetics, and most importantly reduces the amount of absorbed hydrogen. In addition, it should be noted that, even in the cases when the sorption–desorption kinetics was enhanced and the amount of absorbed hydrogen was increased due to changes in the methods of alloy fabrication, in practice, their use remains quite limited due to the high cost of these methods and the problems with transition from lab to production scale.

8. Conclusion

An integrated approach to the development of hydrogen battery materials based on $TiMn_2$ intermetallide allows varying the hydrogen capacity and kinetic parameters of hydrogen sorption–desorption in wide ranges. This approach includes deviation from stoichiometry, additional alloying, change of phase and structural state with or without preliminary heat treatment, and change of the method of alloy production.

REFERENCES

1. K.T. Moller, T.R. Jensen, E. Akiba, and H.W. Li., *Prog. Nat. Sci.*, **27**: 34 (2017); https://doi.org/10.1016/j.pnsc.2016.12.014
2. V.N. Verbetsky and S.V. Mitrokhin, *Materialovedenie*, **1**: 48 (2009) (in Russian).
3. B.P. Tarasov, *Rus. Chem. Journal*, **L**, No. 6: 11 (2006).
4. J. Bellosta von Colbe, J.-R. Ares, J. Barale, M. Baricco, C. Buckley, G. Capurso, N. Gallandat, D.M. Grant, M.N. Guzik, I. Jacob, E.H. Jensen, T. Jensen, J. Jepsen, T. Klassen, M.V. Lototskyy, K. Manickam, A. Montone, J. Puszkiel, S. Sartori, D.A. Sheppard, A. Stuart, G. Walker, C.J. Webb, H. Yang, V. Yartys, A. Züttel, and M. Dornheim, *Int. J. Hydrogen Energy*, **44**: 7780 (2019); https://doi.org/10.1016/j.ijhydene.2019.01.104
5. B.P. Tarasov and M.V. Lototskyy, *Rus. Chem. Journal*, **L**, No. 4: 11 (2006).
6. O. Baklitskaya-Kameneva, *Russian Nanotechnology*, **84**: 14 (2009) (in Russian).
7. B. Viswanathan, *Energy Sources: Fundamentals of Chemical Conversion Processes and Applications* (Elsevier: 2017), Ch. 10, p. 185; https://doi.org/10.1016/B978-0-444-56353-8.00010-1
8. M.V. Lototskyy, *Int. J. Hydrogen Energy*, **41**: 2739 (2016); https://doi.org/10.1016/j.ijhydene.2015.12.055
9. C. Fiori, A. Dell'Era, F. Zuccari, A. Santiangeli, A. D'Orazio, and F. Orecchini, *Int. J. Hydrogen Energy*, **40**: 11879 (2015); https://doi.org/10.1016/j.ijhydene.2015.02.105
10. P. Fragiacomo and F. Piraino, *J. Energy Storage*, **17**: 474 (2018); https://doi.org/10.1016/j.est.2018.04.011
11. L. Gong, Q. Duan, L. Jiang, K. Jin, and J. Sun, *Fuel*, **182**: 419 (2016); https://doi.org/10.1016/j.fuel.2016.05.127
12. M.B. Ley, L.H. Jepsen, Y.S. Lee, Y.W. Cho, J.M. Bellosta von Colbe, M. Dornheim, M. Rokni, J.O. Jensen, M. Sloth, Ya. Filinchuk, J.E. Jørgensen, F. Besenbacher, and T.R. Jensen, *Mater. Today*, **17**, No. 3: 122 (2014); https://doi.org/10.1016/j.mattod.2014.02.013
13. C. Corgnale, B.J. Hardy, and D.L. Anton, *Int. J. Hydrogen Energy*, **37**: 14223 (2012); https://doi.org/10.1016/j.ijhydene.2012.06.040
14. D. Parra, M. Gillott, and G.S. Walker, *Int. J. Hydrogen Energy*, **41**: 5215 (2016); https://doi.org/10.1016/j.ijhydene.2016.01.098
15. D.J. Durbin and C. Malardier-Jugroot, *Int. J. Hydrogen Energy*, **38**: 14595 (2013); https://doi.org/10.1016/j.ijhydene.2013.07.058
16. Z.J. Cao, L.Z. Ouyang, H. Wang, J.W. Liu, L.X. Sun, and M. Zhu, *J. Alloy Compd.*, **639**: 452 (2015); https://doi.org/10.1016/j.jallcom.2015.03.196

17. Z.J. Cao, L.Z. Ouyang, H. Wang, J.W. Liu, D.L. Sun, Q.A. Zhang, and M. Zhu, *Int. J. Hydrogen Energy*, **40**: 2717 (2015); https://doi.org/10.1016/j.ijhydene.2014.12.093
18. H. Barthelemy, M. Weber, and F. Barbier, *Int. J. Hydrogen Energy*, **42**: 7254 (2017); https://doi.org/10.1016/j.ijhydene.2016.03.178
19. *Handbook of Hydrogen Storage: New Materials for Future Energy Storage* (Ed. M. Hirscher) (Wiley-VCH Verlag GmbH & Co. KGaA: 2010); https://doi.org/10.1002/9783527629800
20. R.A. Varin, T. Czujko, and Z.S. Wronski, *Nanomaterials for Solid State Hydrogen Storage* (Berlin: Springer: 2009); https://doi.org/10.1007/978-0-387-77712-2
21. P. Chen and M. Zhu, *Mater. Today*, **11**: 36 (2008); https://doi.org/10.1016/S1369-7021(08)70251-7
22. S.S. Srinivasan and D.E. Demirocak, *Nanostructured Materials for Next-Generation Energy Storage and Conversion: Hydrogen Production, Storage, and Utilization* (Eds. Y.-P. Chen, S. Bashir, and J.L. Liu) (Berlin: Springer: 2017), p. 225; https://doi.org/10.1007/978-3-662-53514-1
23. G. Principi, F. Agresti, A. Maddalena, and S.L. Russo, *Energy*, **34**: 2087 (2009); https://doi.org/10.1016/j.energy.2008.08.027
24. T.P. Chernyaeva and A.V. Ostapov, *Problems Atomic Sci. Technol.*, **5**: 16 (2013) (in Russian).
25. T.M. Roshchina, *Soros Educational J.*, **2**: 89 (1998) (in Russian).
26. A. Zuttel, A. Borgschulte, and L. Schlapbach, *Hydrogen as a Future Energy Carrier* (Wiley-VCH Verlag GmbH & Co. KGaA: 2008); https://doi.org/10.1002/9783527622894
27. A. Zuttel, *Mater. Today*, **6**, No. 9: 24 (2003); https://doi.org/10.1016/S1369-7021(03)00922-2
28. M. Dornheim, *Thermodynamics–Interaction Studies–Solids, Liquids and Gases* (Ed. J.C. Moreno-Piraján) (IntechOpen: 2011), Ch. 33, p. 891; https://doi.org/10.5772/21662
29. V.A. Yartys, V.V. Burnashev, and K.N. Semenenko, *USSR Academy of Sciences. Advances in Chemistry*, **LII**, No. 4: 529 (1983) (in Russian).
30. B.P. Tarasov, M.V. Lototskyy, and V.A. Yartys, *Rus. Chem. Journal*, **L**, No. 6: 34 (2006).
31. R. Griessen, *The Lecture 'Science and Technology of Hydrogen in Metals', IX Chapter: Sustainability and Hydrogen* (Amsterdam: Vrije Universiteit: 2008).
32. A.C. Switendick, *J. Less-Common Met.*, **130**: 249 (1987); https://doi.org/10.1016/0022-5088(87)90116-0
33. A.C. Switendick, *Solid State Commun.*, **8**, No. 15: 1463 (1970); https://doi.org/10.1016/0038-1098(70)90720-9
34. M. Gupta, *J. Less-Common Met.*, **103**: 325 (1984); https://doi.org/10.1016/0022-5088(84)90256-X
35. W.E. Wallace and S.K. Malik, *Hydrides for Energy Storage* (Eds. A.F. Andresen and A.J. Maelands) (New York: Pergamon: 1978), p. 33.
36. H. Smithson, C.A. Marianetti, D. Morgan, A. Van der Ven, A. Predith, and G. Ceder, *Phys. Rev. B*, **66**, No. 12: 144107 (2002); https://doi.org/10.1103/PhysRevB.66.144107
37. Y. Ohsumi, *Hydrogen Absorbing Alloy–Property and Application* (AGNE: 1993) (in Japanese).
38. K. Ohnishi, *The Latest Technologies of Hydrogen-Absorbing Alloys* (CMC: (1994) (in Japanese).

39. V.N. Verbetsky and S.V. Mitrokhin, *Alternative Energy and Ecology*, **10**: 20 (2005) (in Russian).
40. V.A. Yartys, M.V. Lototskyy, E. Akiba, R. Albert, and V.E. Antonov, *Int. J. Hydrogen Energy*, **44**: 7809 (2019); https://doi.org/10.1016/j.ijhydene.2018.12.212
41. N. Gérard and S. Ono, *Hydrogen in Intermetallic Compounds II. Topics in Applied Physics. Vol. **67*** (Berlin–Heidelberg: Springer: 2005), Ch. 4, p. 165; https://doi.org/10.1007/3-540-54668-5_11
42. A. Zaluska, L. Zaluski, and J.O. Ström-Olsen, *J. Alloys Compd.*, **288**: 217 (1999); https://doi.org/10.1016/S0925-8388(99)00073-0
43. V. Skripnyuk, E. Buchman, E. Rabkin, Y. Estrin, M. Popov, and S. Jorgensen, *J. Alloys Compd.*, **436**: 99 (2007); https://doi.org/10.1016/j.jallcom.2006.07.030
44. M. Krystian, M.J. Zehetbauer, H. Kropik, B. Mingler, and G. Krexner, *J. Alloys Compd.*, **509**: S449 (2011); https://doi.org/10.1016/j.jallcom.2011.01.029
45. C. Chiu, S.-J. Huang, T.-Y. Chou, and E. Rabkin, *J. Alloys Compd.*, **743**: 437 (2018); https://doi.org/10.1016/j.jallcom.2018.01.412
46. Z. Dehouche, H.A. Peretti, S. Hamoudi, Y. Yoo, and K. Belkacemi, *J. Alloys Compd.*, **455**: 432 (2008); https://doi.org/10.1016/j.jallcom.2007.01.138
47. M. Felderhoff and B. Bogdanović, *Int. J. Mol. Sci.*, **10**: 325 (2009); https://doi.org/10.3390/ijms10010325
48. C. Zhou, Z.Z. Fang, and R.C. Bowman Jr., *J. Phys. Chem. C*, **119**: 22261 (2015); https://doi.org/10.1021/acs.jpcc.5b06190
49. V.A. Livanov, A.A. Bukhanova, and B.A. Kolachev, *Hydrogen in Titanium* (Moscow: State Scientific and Technical Publishing House of Literature on Ferrous and Non-Ferrous Metallurgy: 1962) (in Russian).
50. T.V. Pryadko, *Metallofiz. Noveishie Tekhnol.*, **37**, No. 2: 243 (2015) (in Russian); https://doi.org/10.15407/mfint.37.02.0243
51. O.I. Dekhtyar, O.M. Ivasishin, D.Yu. Kovalev, O.M. Korduban, V.K. Prokudina, V.I. Ratnikov, D.G. Savvakin, A.Ye. Sychev, and M.M. Gumenyak, *Metallofiz. Noveishie Tekhnol.*, **36**, No. 9: 1153 (2014) (in Russian); https://doi.org/10.15407/mfint.36.09.1153
52. O.M. Ivasyshyn and D.G. Savvakin, *Mater. Sci.*, **51**: 465 (2016); https://doi.org/10.1007/s11003-016-9863-y
53. O.M. Ivasishin, D.G. Savvakin, and N.M. Gumenyak, *Metallofiz. Noveishie Tekhnol.*, **33**, No. 7: 899 (2011) (in Russian).
54. C. Song, L.E. Klebnoff, T.A. Johson, B.S. Chao, A.F. Socha, J.M. Oros, C.J. Radley, S. Wingert, and J.S. Breit, *Int. J. Hydrogen Energy*, **39**: 14896 (2014); https://doi.org/10.1016/j.ijhydene.2014.07.069
55. M.V. Lototskyy, I. Tolj, M.W. Davids, Y.V. Klochko, A. Parsons, D. Swanepoel, R. Ehlers, G. Louw, B. van der Westhuizen, F. Smithd, B.G. Pollet, C. Sita, and V. Linkov, *Int. J. Hydrogen Energy*, **41**: 13831 (2016); https://doi.org/10.1016/j.ijhydene.2016.01.148
56. V.G. Ivanchenko, V.A. Dekhtyarenko, and T.V. Pryadko, *Powder Metall. Met. Ceram.*, **52**: 340 (2013); https://doi.org/10.1007/s11106-013-9531-9
57. S. Satyapal, J. Petrovic, C. Read, G. Thomas, and G. Ordaz, *Catal. Today*, **120**, Nos. 3–4: 246 (2007); https://doi.org/10.1016/j.cattod.2006.09.022

58. A. Godula-Jopek, *Hydrogen Production by Electrolysis* (Ed. A. Godula-Jopek) (Wiley-VCH Verlag GmbH & Co. KGaA: 2015), p. 273;
https://doi.org/10.1002/9783527676507
59. M.V. Lototskyy, I. Tolj, L. Pickering, C. Sita, F. Barbir, and V. Yartys, *Prog. Nat. Sci.*, **27**: 3 (2017);
https://doi.org/10.1016/j.pnsc.2017.01.008
60. M.V. Lototskyy, I. Tolj, A. Parsons, F. Smith, C. Sita, and V. Linkov, *J. Power Sources*, **316**: 239 (2016);
https://doi.org/10.1016/j.jpowsour.2016.03.058
61. A. Narvaez, *Low Cost Metal Hydride-Based Hydrogen Storage System for Forklift Applications (Phase II). Hawaii Hydrogen Carriers, US DOE Annual Merit Review Meeting, June 18, 2014*;
https://www.hydrogen.energy.gov/pdfs/review14/st095_narvaez_2014_p.pdf
62. B.P. Tarasov, M.S. Bocharnikov, Y.B. Yanenko, P.V. Fursikov, and M.V. Lototskyy, *Int. J. Hydrogen Energy*, **43**: 4415 (2018);
https://doi.org/10.1016/j.ijhydene.2018.01.086
63. L.E.R. Vega, D.R. Leiva, R.M. Leal Neto, W.B. Silva, R.A. Silva, T.T. Ishikawa, C.S. Kiminami, and W.J. Botta, *Int. J. Hydrogen Energy*, **43**, No. 5: 2913 (2018);
https://doi.org/10.1016/j.ijhydene.2017.12.054
64. V.Yu. Zadorozhnyy, G.S. Milovzorov, S.N. Klyamkin, M.Yu. Zadorozhnyy, D.V. Strugova, M.V. Gorshenkov, and S.D. Kaloshkina, *Prog. Nat. Sci.: Materials Int.*, **27**, No. 1: 149 (2017);
https://doi.org/10.1016/j.pnsc.2016.12.008
65. L. Pickering, M.V. Lototskyy, M.W. Davids, C. Sita, and V. Linkov, *Mater Today: Proc.*, **5**: 10470 (2018);
https://doi.org/10.1016/j.matpr.2017.12.378
66. M. Shibuya, J. Nakamura, and E. Akiba, *J. Alloys Compd.*, **466**: 558 (2018);
https://doi.org/10.1016/j.jallcom.2007.11.120
67. P. Lv, Z. Liu, A. K. Patel, X. Zhou, and J. Huot, *Metals Materials Intl.*, **26**: 205 (2020);
https://doi.org/10.1007/s12540-019-00501-1
68. P. Lv and J. Huot, *Int. J. Hydrogen Energy*, **41**: 22128 (2016);
https://doi.org/10.1016/j.ijhydene.2016.07.091
69. H. Leng, Z. Yu, J. Yin, Q. Li, Z. Wu, and K.-C. Chou, *Int. J. Hydrogen Energy*, **42**: 23731 (2017);
https://doi.org/10.1016/j.ijhydene.2017.01.194
70. E.I. Gkanas, M. Khzouz, G. Panagakos, T. Statheros, G. Mihalakakou, G.I. Siasos, G. Skodras, and S.S. Makridis, *Energy*, **142**: 518 (2018);
https://doi.org/10.1016/j.energy.2017.10.040
71. M. Lototskyy, I. Tolj, Y. Klochko, M.W. Davids, D. Swanepoel, and V. Linkov, *Int. J. Hydrogen Energy*, **45**: 7958 (2020);
https://doi.org/10.1016/j.ijhydene.2019.04.124
72. Y. Kojima, Y. Kawai, S. Towata, T. Matsunaga, T. Shinozawa, and M. Kimbara, *J. Alloys Compd.*, **419**: 256 (2006);
https://doi.org/10.1016/j.jallcom.2005.08.078
73. J.G. Park, H.Y. Jang, S.C. Han, P.S. Lee, and J.Y. Lee, *Mat. Sci. Eng. A*, **329–331**: 351 (2002);
https://doi.org/10.1016/S0921-5093(01)01598-2
74. S.V. Mitrokhin, T.N. Bezuglaya, and V.N. Verbetsky, *J. Alloys Compd.*, **330–332**: 146 (2002);
https://doi.org/10.1016/S0925-8388(01)01469-4

75. Z. Dehouche, M. Savard, F. Laurencelle, and J. Goyette, *J. Alloys Compd.*, **400**: 276 (2005); https://doi.org/10.1016/j.jallcom.2005.04.007
76. J.L. Bobet and T.B. Darriet, *Int. J. Hydrogen Energy*, **25**, No. 8: 767 (2000); https://doi.org/10.1016/S0360-3199(99)00101-9
77. H. Oesterreicher and H. Bittner, *Mat. Res. Bull.*, **13**: 83 (1978); https://doi.org/10.1016/0025-5408(78)90031-4
78. D.P. Shoemaker and C.B. Shoemaker, *J. Less-Common Met.*, **68**, No. 1: 43 (1979); https://doi.org/10.1016/0022-5088(79)90271-6
79. Y. Morita, T. Gamo, and S. Kuranaka, *J. Alloys Compd.*, **253–254**: 29 (1997); https://doi.org/10.1016/S0925-8388(96)03056-3
80. X. Yu, B. Xia, Z. Wu, and N. Xu, *Mat. Sci. Eng. A*, **373**, Nos. 1–2: 303 (2004); https://doi.org/10.1016/j.msea.2004.02.008
81. V. Ivanchenko and T. Pryadko, *Landolt-Börnstein. New Series. Group IV* (Springer: 2007), vol. **11**, No. 3, p. 475.
82. A. Walnsch, M.J. Kriegel, O. Fabrichnaya, and A. Leineweber, *J. Phase Equilibria Diffusion*, **41**: 457 (2020); https://doi.org/10.1007/s11669-020-00804-6
83. S. Samboshi, N. Masahashi, and S. Hanada, *J. Alloys Compd.*, **352**: 210 (2003); https://doi.org/10.1016/S0925-8388(02)01125-8
84. R.M. Waterstrat, *Trans. Metall. Soc. AIME*, **221**: 686 (1961).
85. V.N. Svechnikov and V.V. Pet'kov, *Metallofizika*, **64**: 24 (1976) (in Russian).
86. V. Ivanchenko, V. Dekhtyarenko, T. Kosorukova, and T. Pryadko, *Chem. Metals Alloys.*, **1**, No. 2: 137 (2008); https://doi.org/10.30970/cma1.0045
87. T. Yamashita, T. Gamo, Y. Moriwaki, and M. Fukuda, *Nippon Kinzoku Gakkaishi–Journal of the Japan Institute of Metals*, **41**: 148 (1977).
88. S. Samboshi, N. Masahashi, and S. Hanada, *Acta Mater.*, **49**: 927 (2001) https://doi.org/10.1016/S1359-6454(00)00371-2
89. X.Y. Song, Y. Chen, Z. Zhang, Y.Q. Lei, X.B. Zhang, and Q.D. Wang, *Int. J. Hydrogen Energy*, **25**: 649 (2000); https://doi.org/10.1016/S0360-3199(99)00080-4
90. N. Bouaziz, M. Bouzid, and A.B. Lamine, *Int. J. Hydrogen Energy*, **43**: 1615 (2018); https://doi.org/10.1016/j.ijhydene.2017.11.049
91. T. Huang, Z. Wu, G. Sun, and N. Xu, *Intermetallics*, **15**: 593 (2007); https://doi.org/10.1016/j.intermet.2006.10.035
92. V.A. Dekhtyarenko, *Regularities and Mechanisms of Interaction of Hydrogen with Multicomponent Titanium Alloys Based on Laves Phases and B.C.C. Solid Solution* (Abstract of a Thesis. for Dr. Tech. Sci.) (Kyiv: G.V. Kurdyumov Institute for Metal Physics, N.A.S.U.: 2021) (in Ukrainian).
93. M. Yoshida and E. Akiba, *J. Alloys Compd.*, **224**, No. 1: 121 (1995); https://doi.org/10.1016/0925-8388(95)01518-3
94. A. Ming, F. Pourarian, S.G. Sankar, W.E. Wallace, and L. Zhang, *Mater. Sci. Eng.*, **33**: 53 (1995).
95. B.H. Liu, D.M. Kim, K.Y. Lee, and J.Y. Lee, *J. Alloys Compds.*, **240**, Nos. 1–2: 214 (1996); https://doi.org/10.1016/0925-8388(96)02245-1
96. H. Taizhong, W. Zhu, Y. Xuebin, C. Jinzhou, X. BaoJia, H. Tiesheng, and X. Naixin, *Intermetallics*, **12**, No. 1: 91 (2004); https://doi.org/10.1016/j.intermet.2003.08.005

97. V.G. Ivanchenko, V.I. Nichiporenko, and T.V. Pryadko, *Metallofiz. Noveishie Tekhnol.*, **28**: 977 (2006) (in Russian).
98. V.G. Ivanchenko, T.V. Pryadko, I.S. Gavrylenko, and V.V. Pogorelaya, *Chem. Met. Alloys*, **1**, No. 1: 67 (2008); https://doi.org/10.30970/cma1.0004
99. I. Jacob, A. Stern, A. Moran, D. Shaltiel, and D. Davidov, *J. Less-Common Met.*, **73**: 369 (1980); https://doi.org/10.1016/0022-5088(80)90331-8
100. H.-H. Lee, K.-Y. Lee, and J.-Y. Lee, *J. Alloys Compd.*, **239**: 63 (1996); https://doi.org/10.1016/0925-8388(96)02276-1
101. C.E. Lundin, F.E. Lynca, and C.B. Magee, *J. Less-Common Met.*, **56**: 19 (1977); https://doi.org/10.1016/0022-5088(77)90215-6
102. J.G. Park, H.Y. Jang, S.C. Han, P.S. Lee, and J.Y. Lee, *J. Alloys Compd.*, **325**: 293 (2001); https://doi.org/10.1016/S0925-8388(01)01409-8
103. Y. Wang, Y. Zhang, X. Wang, and C. Chen, *Acta Metallurgica Sinica*, **42**, No. 6: 641 (2006).
104. G. Li, N. Nishimiya, H. Satoh, and N. Kamegashira, *J. Alloys Compd.*, **393**: 231 (2005); https://doi.org/10.1016/j.jallcom.2004.08.097
105. A.A. Shkola, *Metallofiz. Noveishie Tekhnol.*, **38**, No. 9: 1213 (2016) (in Ukrainian); https://doi.org/10.15407/mfint.38.09.1213
106. A.V. Revyakin and V.A. Reznichenko, *Titanium and Its Alloys. Issue II. Metallurgy of Titanium* (Moscow: Publishing House of the Academy of Sciences of the U.S.S.R.: 1959) (in Russian).
107. G.F. Kobzenko, A.A. Shkola, and T.V. Pryadko, *Metallofiz. Noveishie Tekhnol.*, **24**, No. 12: 1679 (2002) (in Russian).
108. R.L. Kurtz and V.E. Henrich, *Phys. Rev. B*, **26**, No. 12: 6682 (1982); https://doi.org/10.1103/PhysRevB.26.6682
109. J.R. Johnson, *J. Less-Common Met.*, **73**: 345 (1980); https://doi.org/10.1016/0022-5088(80)90328-8
110. J. Bodega, J.F. Fernández, F. Leardini, J.R. Ares, and C. Sánchez, *J. Physics Chem. Solids*, **72**, No. 11: 1334 (2011); https://doi.org/10.1016/j.jpcs.2011.08.004
111. E.A. Anikina and V.N. Verbetsky, *Int. J. Hydrogen Energy*, **36**: 1344 (2011); https://doi.org/10.1016/j.ijhydene.2010.06.085
112. S.V. Mitrokhin, T.N. Smirnova, V.A. Somenkov, V.P. Glazkov, and V.N. Verbetsky, *J. Alloys Compd.*, **356–357**: 80 (2003); https://doi.org/10.1016/S0925-8388(03)00257-3
113. V.A. Dekhtyarenko, *Metallofiz. Noveishie Tekhnol.*, **37**, No. 7: 683 (2015) (in Russian); https://doi.org/10.15407/mfint.37.05.0683
114. T.V. Pryadko and V.A. Dekhtyarenko, *Metallofiz. Noveishie Tekhnol.*, **40**, No. 5: 649 (2018) (in Russian); https://doi.org/10.15407/mfint.40.05.0649
115. V.A. Dekhtyarenko, *Metallofiz. Noveishie Tekhnol.*, **41**, No. 10: 1283 (2019); https://doi.org/10.15407/mfint.41.10.1283
116. X.B. Yu, J.Z. Chen, Z. Wu, B.J. Xia, and N.X. Xu, *Int. J. Hydrogen Energy*, **29**: 1377 (2004); https://doi.org/10.1016/j.ijhydene.2004.01.015

117. R.R. Jeng, C.Y. Chou, S.-L. Lee, Y.C. Wu, and H.Y. Bor, *J. Chinese Institute Engineers*, **34**. No. 5: 601 (2011).
118. B. Predel, *Phase Equilibria, Crystallographic and Thermodynamic Data of Binary Alloys Cr–Cs ... Cu–Zr* (Ed. O. Madelung), Ch. 1, p. 1 (Berlin–Heidelberg: Springer-Verlag: 1994); https://doi.org/10.1007/10086090_1030
119. K.N. Young and J. Nei, *Materials (Basel)*, **6**, No. 10: 4574 (2013); https://doi.org/10.3390/ma6104574
120. T.P. Yadav, R.R. Shahi, and O.N. Srivastava, *Int. J. Hydrogen Energy*, **37**: 3689 (2012); https://doi.org/10.1016/j.ijhydene.2011.04.210
121. F. Stein, M. Palm, and G. Sauthoff, *Intermetallics*, **12**. Nos. 7–9, Spec. Iss.: 713 (2004); https://doi.org/10.1016/j.intermet.2004.02.010
122. D.J. Thoma and J.H. Perepezko, *J. Alloys Compd.*, **224**, No. 2: 330 (1995); https://doi.org/10.1016/0925-8388(95)01557-4
123. S.V. Mitrokhin, T.N. Bezuglaya, and V.N. Verbetsky, *Hydrogen Energy Progress XIII: Proceedings of the 13th World Hydrogen Energy Conference (Beijing, China, June 12–15, 2000)*, p. 534.
124. P. Liu, X. Xie, L. Xu, X. Li, and T. Liu, *Prog. Natur. Sci.: Mat. Int.*, **27**: 652 (2017); https://doi.org/10.1016/j.pnsc.2017.09.007
125. N.N. Greenwood and A. Earnshaw, *Chemistry of the Elements. 2nd Ed.* (Oxford: Butterworth Heinemann: 1997).
126. Z. Cao, L. Ouyang, H. Wang, J. Liu, L. Sun, and M. Zhu, *J. Alloys Compd.*, **639**: 452 (2015); https://doi.org/10.1016/j.jallcom.2015.03.196
127. H. Iba and E. Akiba, *J. Alloys Compd.*, **253–254**: 21 (1997); https://doi.org/10.1016/S0925-8388(96)03072-1
128. E. Akiba and H. Iba, *Intermetallics*, **6**: 461 (1998); https://doi.org/10.1016/S0966-9795(97)00088-5
129. V.G. Ivanchenko, V.A. Dekhtyarenko, and T.V. Pryadko, *Metallofiz. Noveishie Tekhnol.*, **33**, Spec. Iss: 479 (2011) (in Russian).
130. V.G. Ivanchenko, V.A. Dekhtyarenko, T.V. Pryadko, and I.I. Mel'nik, *Metallofiz. Noveishie Tekhnol.*, **35**, No. 11: 1465 (2013) (in Russian).
131. V. Dekhtyarenko, T. Pryadko, and O. Boshko, *Chem. Metals Alloys*, **11**: 77 (2018); https://doi.org/10.30970/cma11.0371
132. G.G. Libowitz and A. Maeland, *Material Science Forum*, **30**: 177 (2015); https://doi.org/10.4028/www.scientific.net/MSF.31.177
133. S. Ono, K. Nomura, and J. Ikeda, *J. Less-Common. Met.*, **72**, No. 2: 159 (1980); https://doi.org/10.1016/0022-5088(80)90135-6
134. K. Ohnishi and T. Kabutomori, *The Latest Technologies of Hydrogen Absorbing Alloys* (CMC: 1994), p. 33.
135. J. Huot, D.B. Ravnsbæk, J. Zhang, F. Cuevas, M. Latroche, and T.R. Jensen, *Prog. Mater. Sci.*, **58**: 30 (2013); https://doi.org/10.1016/j.pmatsci.2012.07.001
136. C. Raufast, D. Plante, and S. Miraglia, *J. Alloys Compd.*, **617**: 633 (2014); https://doi.org/10.1016/j.jallcom.2014.07.089
137. N. Skryabina, D. Fruchart, M.G. Shelyapina, S. Dolukhanyan, and A. Aleksanyan, *J. Alloys Compd.*, **580**: S94 (2013); https://doi.org/10.1016/j.jallcom.2013.03.114

138. H. Itoh, H. Arashima, K. Kubo, T. Kabutomori, and K. Ohnishi, *J. Alloys Compd.*, **404–406**: 417 (2005); https://doi.org/10.1016/j.jallcom.2004.12.175
139. V.A. Dekhtyarenko, T.V. Pryadko, D.G. Savvakin, V.I. Bondarchuk, and G.S. Mogylnyy, *Int. J. Hydrogen Energy*, **46**: 8040 (2021); https://doi.org/10.1016/j.ijhydene.2020.11.283
140. R.R. Chen, X.Y. Chen, X. Ding, X.Z. Li, J.J. Guo, H.S. Ding, Y.Q. Su, and H.Z. Fu, *J. Alloys Compd.*, **748**: 171 (2018); https://doi.org/10.1016/j.jallcom.2018.03.154
141. S. Suwarno, J.K. Solberg, J.P. Maehlen, B. Krogh, and V.A. Yartys, *Int. J. Hydrogen Energy*, **37**: 7624 (2012); https://doi.org/10.1016/j.ijhydene.2012.01.149
142. S. Suwarno, J.K. Solberg, J.P. Maehlen, B. Krogh, B.T. Børresen, E. Ochoa-Fernandez, E. Rytter, M. Williams, R. Denys, and V.A. Yartys, *Trans. Nonferrous Metals Soc. China*, **22**, No. 8: 1831 (2012); https://doi.org/10.1016/S1003-6326(11)61394-0
143. J. Matsuda and E. Akiba, *J. Alloy Compd.*, **581**: 369 (2013); https://doi.org/10.1016/j.jallcom.2013.07.073
144. M. Balcerzak, *Int. J. Hydrogen Energy*, **42**: 23698 (2017); https://doi.org/10.1016/j.ijhydene.2017.03.224
145. J.F. Lynch, A.J. Maeland, and G.G. Libowitz, *Z. Phys. Chem.*, **145**, No. 12: 51 (1985); https://doi.org/10.1524/zpch.1985.145.1_2.051
146. V. Ivanchenko, T. Pryadko, V. Dekhtyarenko, and T. Kosorukova, *Chem. Metals Alloys.*, **1**, No. 2: 133 (2008); https://doi.org/10.30970/cma1.0044
147. V.G. Ivanchenko, V.A. Dekhtyarenko, and T.V. Pryadko, *Metal Sci. Treatment Metals.*, **1**: 4 (2010) (in Ukrainian);
148. V.A. Dekhtyarenko, *Metallofiz. Noveishie Tekhnol.*, **36**, No. 3: 375 (2014) (in Russian); https://doi.org/10.15407/mfint.36.03.0375
149. V.G. Ivanchenko, V.A. Dekhtyarenko, and T.V. Pryadko, *Metallofiz. Noveishie Tekhnol.*, **37**, No. 4: 521 (2015); https://doi.org/10.15407/mfint.37.04.0521
150. V.A. Dekhtyarenko, *Mater. Sci. Non-Equilibrium Phase Transform.*, **5**, No. 3: 78 (2019).
151. V.A. Dekhtyarenko, T.V. Pryadko, D.G. Savvakin, and T.A. Kosorukova, *Metallofiz. Noveishie Tekhnol.*, **41**, No. 11: 649 (2019) (in Russian); https://doi.org/10.15407/mfint.41.11.1455
152. T.V. Pryadko, V.A. Dekhtyarenko, K.M. Khranovs'ka, and H.S. Mohyl'nyi, *Mater. Sci.*, **55**, No. 6: 854 (2020); https://doi.org/10.1007/s11003-020-00379-0
153. G.P. Grabovetskaya, N.N. Nikitenkov, I.P. Mishin, I.V. Dushkin, and E.N. Stepanova, *Bulletin Tomsk Polytech. Univ.*, **323**: 55 (2013) (in Russian).
154. Z.A. Matysina and D.A. Schur, *Hydrogen and Solid-Phase Transformations in Metals, Alloys and Fullerites* (Dnipro: Science and Education: 2002) (in Russian).
155. D.H. Savvakin, M.M. Humenyak, M.V. Matviychuk, and O.H. Molyar, *Mater. Sci.*, **47**: 651 (2012); https://doi.org/10.1007/s11003-012-9440-y
156. *Gase und Kohlenstoff in Metallen. Reine und angewandte Metallkunde in Einzeldarstellungen* (Hrsg. E. Fromm und E. Gebhardt) (Berlin–Heidelberg–

New York: Springer Verlag: 1976), Bd. **26** (in German);
https://doi.org/10.1002/bbpc.19770810821
157. K. Young, K. Young, T. Ouchi, B. Huang, B. Chao, M.A. Fetcenko, L.A. Bendersky, K. Wang, and C. Chiu, *J. Alloys Compd.*, **506**, No. 2: 841 (2010);
https://doi.org/10.1016/j.jallcom.2010.07.091
158. V.G. Ivanchenko, V.A. Dekhtyarenko, T.V. Pryadko, D.G. Savvakin, and I.K. Evlash, *Mater. Sci.*, **51**, No. 4: 492 (2015);
https://doi.org/10.1007/s11003-016-9867-7
159. X. Liu, L. Jiang, Z. Liu, Z. Huang, and S. Wang, *J. Alloys Compd.*, **471**, Nos. 1–2: L36 (2009);
https://doi.org/10.1016/j.jallcom.2008.04.004
160. A. Gueguen, J.M. Joubert, and M. Latroche, *J. Alloys Compd.*, **509**, No. 6: 3013 (2011);
https://doi.org/10.1016/j.jallcom.2010.10.213
161. Z. Hang, X. Xiao, S. Li, H. Ge, C. Chen, and L. Chen, *J. Alloys Compd.*, **529**: 128 (2012);
https://doi.org/10.1016/j.jallcom.2012.03.044
162. H.Y. Zhou, F. Wang, J. Wang, Z.M. Wang, Q.R. Yao, J.Q. Deng, C.Y. Tang, and G.H. Rao, *Int. J. Hydrogen Energy*, **39**: 14887 (2014);
https://doi.org/10.1016/j.ijhydene.2014.07.054
163. K. Young, T. Ouchi, J. Nei, and L. Wang, *J. Alloys Compd.*, **654**: 216 (2016);
https://doi.org/10.1016/j.jallcom.2015.09.010
164. K. Young, T. Ouchi, J. Nei, and T. Meng, *J. Power Sources.*, **281**: 164 (2015);
https://doi.org/10.1016/j.jpowsour.2015.01.170
165. M. Enomoto, *J. Phase Equilibria*, **13**: 195 (1992).
166. W.B. Pearson and J.W. Christian, *Acta Cryst.*, **5**: 157 (1952);
https://doi.org/10.1107/S0365110X52000484
167. A.A. Kodentzov, S.F. Dunaev, and E.M. Slusarenko, *J. Less-Comm. Met.*, **135**: 15 (1987);
https://doi.org/10.1016/0022-5088(87)90334-1
168. J.-M. Joubert, R. Černý, M. Latroche, E. Leroy, L.Guénée, A. Percheron-Guégan, and K. Yvon, *J. Solid State Chem.*, **166**, No. 1: 1 (2002);
https://doi.org/10.1006/jssc.2001.9499
169. C. Jordy, M. Latroche, A. Percheron-Guégan, and J.C. Achard, *Z. Phys. Chem.*, **185**: 119 (1994).
170. Q.A. Zhang, Y.Q. Lei, C.S. Wang, F.S. Wang, and Q.D. Wang, *J. Power Sources*, **75**, No. 2: 288 (1998);
https://doi.org/10.1016/S0378-7753(98)00112-8
171. P. Pei, X.P. Song, J. Liu, G.L. Chen, X.B. Qin, and B.Y. Wang, *Int. J. Hydrogen Energy*, **34**, No. 19: 8094 (2009);
https://doi.org/10.1016/j.ijhydene.2009.08.023
172. J.H. Kim, H. Lee, K.T. Hwang, and J.S. Han, *Int. J. Hydrogen Energy*, **34**, No. 23: 9424 (2009);
https://doi.org/10.1016/j.ijhydene.2009.09.087
173. H. Kazemipour, A. Salimijazi, A. Saidi, A. Saatchi, and A. Aref arjmand, *Int. J. Hydrogen Energy*, **3**, Iss. 24: 12784 (2014);
https://doi.org/10.1016/j.ijhydene.2014.06.085
174. S. Suwarno, J.K. Solberg, V.A. Yartys, and B. Krogh, *J. Alloys Compd.*, **509**, Suppl. 2: S775 (2011);
https://doi.org/10.1016/j.jallcom.2010.10.130
175. I.P. Jain, P. Jain, and A. Jain, *J. Alloys Compd.*, **503**, No. 2: 303 (2010);
https://doi.org/10.1016/j.jallcom.2010.04.250

176. A. Kumar, K. Shashikala, S. Banerjee, J. Nuwad, P. Das, and C.G.S. Pillai, *Int. J. Hydrogen Energy*, **37**, No. 4: 3677 (2012); https://doi.org/10.1016/j.ijhydene.2011.04.135
177. P. Pei, X.P. Song, J. Liu, M. Zhao, and G.L. Chen, *Int. J. Hydrogen Energy*, **34**, No. 20: 8597 (2009); https://doi.org/10.1016/j.ijhydene.2009.08.038
178. C.Y. Seo, J.H. Kim, P.S. Lee, and J.Y. Lee, *J. Alloys Compd.*, **348**, Nos. 1–2: 252 (2003); https://doi.org/10.1016/S0925-8388(02)00831-9

Received 18.06.2021;
in final version, 25.06.2021

В.А. Дехтяренко, Д.Г. Саввакін, В.І. Бондарчук, В.М. Шиванюк, Т.В. Прядко, О.О. Стасюк

Інститут металофізики ім. Г.В. Курдюмова НАН України, бульв. Академіка Вернадського, 36; 03142 Київ, Україна

СТОПИ НА ОСНОВІ ІНТЕРМЕТАЛІДУ $TiMn_2$
ДЛЯ АКУМУЛЯЦІЇ ВОДНЮ: ПРОБЛЕМИ ТА ПЕРСПЕКТИВИ

Визначено основні переваги водню як енергоносія порівняно з використовуваними на даний час вуглеводнями. Зіставлянням переваг та недоліків наявних на сьогодні методів зберігання водню доведено, що зберігання його у зв'язаному стані (гідриди) має найбільшу кількість запасеного водню на одиницю маси контейнера і є найбезпечнішим. Показано, що стопи на основі інтерметаліду типу AB_2 є найперспективнішими матеріалами для безпечного зберігання та транспортування водню у зв'язаному стані.

Ключові слова: водень, гідриди, Лавесова фаза, гідрування, дегідрування, воднева місткість.